2-21-1992

Network Analysis of Intermediary Metabolism Using Linear Optimization. I. Development of Mathematical Formalism

Joanne M. (Savinell) Belovich
Cleveland State University

Bernhard O. Palsson
University of Michigan

Network Analysis of Intermediary Metabolism using Linear Optimization. I. Development of Mathematical Formalism

JOANNE M. SAVINELL AND BERNHARD O. PALSSON

Analysis of metabolic networks using linear optimization theory allows one to quantify and understand the limitations imposed on the cell by its metabolic stoichiometry, and to understand how the flux through each pathway influences the overall behavior of metabolism. A stoichiometric matrix accounting for the major pathways involved in energy and mass transformations in the cell was used in our analysis. The auxiliary parameters of linear optimization, the so-called shadow prices, identify the intermediates and cofactors that cause the growth to be limited on each nutrient. This formalism was used to examine how well the cell balances its needs for carbon, nitrogen, and energy during growth on different substrates. The relative values of glucose and glutamine as nutrients were compared by varying the ratio of rates of glucose to glutamine uptakes, and calculating the maximum growth rate. The optimum value of this ratio is between 2–7, similar to experimentally observed ratios. The theoretical maximum growth rate was calculated for growth on each amino acid, and the amino acids catabolized directly to glutamate were found to be the optimal nutrients. The importance of each reaction in the network can be examined both by selectively limiting the flux through the reaction, and by the value of the reduced cost for that reaction. Some reactions, such as malic enzyme and glutamate dehydrogenase, may be inhibited or deleted with little or no adverse effect on the calculated cell growth rate.

Introduction

The stoichiometric complexity of intermediary metabolism and its interactions with compounds external to the cell preclude an understanding of the events that affect and modify the cell's metabolic behavior. Improving our understanding of this complex process is both of basic scientific interest as well as of significant practical utility. The set of constraints imposed by the stoichiometry on the distribution of resources through the metabolic network is one aspect of the overall mechanism for cellular control and regulation. Therefore, an improved understanding of the stoichiometry is crucial for greater understanding of the mechanisms that regulate cell behavior. Likewise, when growing cells in culture, one would like to predict how the addition or removal of nutrients or related substances will affect the cell's metabolism. The optimization of process designs and media formulations requires that one know which nutrients are needed, and their necessary quantities, how waste

production and product formation are affected, and the degree to which nutrients are able to substitute for each other. This information may be obtained from network analysis of the cell's metabolism.

The general equation that describes cell metabolism at steady state is given by:

$$\mathbf{S} \cdot \boldsymbol{v}(\boldsymbol{X}) = \boldsymbol{b}$$

where $\mathbf{S}$ is the stoichiometric matrix, $\boldsymbol{v}(\boldsymbol{X})$ is the vector of reaction rates, and $\boldsymbol{b}$ is the vector of consumption and production rates and biosynthetic fluxes. A large body of literature is available discussing the applications of this model equation to different systems, and the emphasis is usually placed on the enzyme mechanisms, given by $\boldsymbol{v}(\boldsymbol{X})$, and the parameters found therein. The emphasis of this present work is on the structure of metabolic network itself, given by the stoichiometric matrix $\mathbf{S}$, instead of the system dynamics. A formalism will be presented which allows one to draw conclusions about the characteristics of cell metabolism, and the role of the stoichiometric structure in determining these characteristics, using only the information in the stoichiometric matrix.

The stoichiometry of the chemical reactions that comprise intermediary metabolism is well-established, although there may be minor variations between cell lines. Stoichiometric coupling between reactions places constraints on the quantities of specific nutrients that are required for growth and metabolism, and thus determines the distribution pattern of the nutrients through the metabolic network. In general, these constraints are fixed, and they thus provide a means for reducing the degree of freedom in the cell from an infinite space of solutions, to a set of fixed algebraic expressions resulting from the mass balances. The goal of this work is to derive as much information as possible about the behavior of the cell from the stoichiometry; no information on reaction rate expressions or kinetic parameters is included in this analysis. The results presented here were calculated assuming that the metabolic network stoichiometry is constant.

Previous work using stoichiometry in biochemical networks has included the derivation of a fermentation equation incorporating mass balance information as an online monitor in fermentations for prediction of experimental data and calculation of product yields (Papoutsakis & Meyer, 1985). Although the fluxes through internal reactions cannot be calculated with this equation, this method does provide a means for testing whether a particular reaction is active in the network, by checking the consistency of experimental measurement with and without the inclusion of the reaction in question. However, consistency of experimental measurements with calculated results does not necessarily imply that the network is correct. This method for compiling mass balance information was improved by the application of Gibbs' rule of stoichiometry (Tsai & Lee, 1988), in which the number of pathway mass balances that can be used in addition to elemental balances was calculated. The resulting system of equations is much smaller, and thus more practical for online monitoring, yet gives the same information as the longer fermentation equation. Gibb's rule of stoichiometry was also used by two research groups, with similar results, to derive a parameter (Tsai & Lee, 1988; Niranjan & San, 1989) which indicates whether an agreement of calculated product yields with experimental data is enough to verify the validity of a proposed network.

The approach used in our present analysis is to formulate mass balances for each major metabolite in the cell, assuming that the network stoichiometry is well-known, and then calculate the steady-state flux through each pathway. The calculation of each flux in the central metabolic pathways has permitted the study of biomass conversion efficiency, and the formation of theories about control of reactions (Walsh & Koshland, 1985; Holms, 1986). Even with detailed mass balances and exact stoichiometry, it is not possible to calculate uniquely each flux, without experimental data, due to the large number of branch points in the metabolic network. Consequently, several researchers have measured the rates of radioactive label incorporation into a number of glycolytic and tricarboxylic acid (TCA) cycle intermediates and products, in order to calculate the fluxes through the entire network, in bacteria (Walsh & Koshland, 1985), protozoa (Blum & Stein, 1982), liver tissue (Sauer *et al.*, 1970; Stucki & Walter, 1972; Crawford & Blum, 1983; Rabkin & Blum, 1985), and heart (Safer & Williamson, 1973). While good estimates of the fluxes may be obtained through these methods, the results are applicable only to the particular experimental conditions, and require a large amount of effort and time.

A more generalized approach for analyzing mass distribution in metabolic networks involves the use of linear optimization techniques. Linear optimization has been applied to adipocyte metabolism (Fell & Small, 1986), to ascertain the role of the pentose phosphate shunt (PPS) in NADPH production and in the production of triglycerides from glucose. Linear programming has also been used to determine the maximum yields of fermentation products from glucose, and whether flux through PPS limits these yields (Papoutsakis & Meyer, 1985). Acetate secretion by *Escherichia coli* has been predicted to occur when ATP production is maximized and flux through particular reactions are limited (Majewski & Domach, 1990). While each of these research groups has found useful results with linear optimization, a comprehensive assessment of the value and limitations of linear optimization as applied to metabolic networks has not been undertaken.

We will extend the use of linear optimization, to examine a range of issues relevant to mammalian cell growth in culture. We will first demonstrate the physical significance of several parameters in linear optimization theory, and how these can be used to improve understanding of metabolic networks. Linear optimization provides a means for comparing the value of different nutrients in terms of their overall growth supporting ability, as well as their ability to satisfy and balance the specific demands of the cell (e.g. energy production, intermediates for biosynthesis). We can identify reactions that are not necessary for cell growth, and which may even inhibit growth, and we can predict how inhibition of certain reactions may affect cell growth. Linear optimization is also used as a tool to study the relationship between competing nutrients, such as glucose and glutamine, with oxygen. The results shown here will be true for transformed cell lines that have metabolic networks similar to the one used here.

The second part of this series (Savinell & Palsson, 1991) will apply linear optimization to the metabolic network of a specific hybridoma cell line under study in our laboratory. It will be used as a means for interpreting experimental measurements of fluxes of metabolites entering and leaving the cell. From these calculations, we will identify the limiting nutrients under particular environmental conditions. We

will also compare the cost of synthesizing intermediates in terms of the nutrients glucose and glutamine.

Mathematical Formulation

Problem statement

The system of equations that describes mass balances for the metabolites is:

$$\frac{d\boldsymbol{X}}{dt} = \mathbf{S} \cdot \boldsymbol{v} - \boldsymbol{b} \tag{1}$$

where $\boldsymbol{X}$ is the vector of metabolite amounts per cell, $\mathbf{S}$ is the $n \times m$ stoichiometric matrix, n is the number of metabolites, $\boldsymbol{v}$ is the vector of m reaction fluxes, and $\boldsymbol{b}$ is the vector of known substrate consumption rates, waste production rates, and biosynthetic fluxes. The element S_{ij} is the stoichiometric coefficient of the ith compound in the jth reaction. If the rate of volume expansion due to growth is slow compared to metabolic transients then we can assume that the following condition

$$\mathbf{S} \cdot \boldsymbol{v} = \boldsymbol{b} \tag{2}$$

holds and that this equation can be used to calculate the steady-state metabolic fluxes.

However, typically the number of rates is greater than the number of mass balances (i.e. $m > n$). Consequently, the stoichiometry of the metabolic network does not uniquely specify the fluxes through the cell's pathways, so that the number of possible flux distributions allowed by the stoichiometry is infinite. The cell's choice of the flux distribution is imbedded in the kinetic characteristics of the enzymes. However, in the absence of detailed knowledge of enzyme kinetics, we can estimate the metabolic flux distribution if we postulate the "objectives" that underlie the cell's behavior. An underdetermined set of equations can be solved uniquely, given an objective function, using linear optimization techniques.

Linear programming

We can thus formulate the solution to eqn (2) as a linear programming problem and use the Simplex algorithm to find a solution (Luenberger, 1984):

$$\text{minimize } Z = \sum c_i \cdot v_i \tag{3}$$

where Z is the objective which is represented as a linear combination (as defined by the weights in the vector c_i) of the fluxes v_i. As we will show later, the representation of Z enables us to formulate physiologically meaningful objective functions.

The optimization in eqn (3) is subject to constraints:

$$\mathbf{S} \cdot \boldsymbol{v} = \boldsymbol{b} \tag{4}$$

$$v_i < \alpha_i, \qquad i = 1, 2, \ldots, m. \tag{5}$$

The first set of constraints is simply that of the steady-state flux balances, from eqn (2). The second set of constraints introduces a vector of parameters, α, which represents the maximum fluxes allowable through reactions v. The value of each parameter α_i is obtained from the *in vitro* measurement of the maximum activity of the enzyme i. This constraint represents the fact that fluxes through each enzymatic reaction are limited by the amount of that enzyme present in the cell, as well as the rate with which the particular enzyme can react with the substrate. However, the *in vivo* regulation of many enzymes may be very different from that observed *in vitro*, and thus the maximum activities must be used with caution and only if the *in vivo* values are well-known. In the results presented here, the parameters in α are set to infinity, unless specifically mentioned.

The solution, $\boldsymbol{v}$, of the linear programming problem will always be non-negative, due to the characteristics of the Simplex algorithm. Consequently, reversible reactions must be formulated as two separate reactions, one in the forward direction, and the other in the reverse direction. This property allows us to incorporate limited thermodynamic information by distinguishing between reversible and non-reversible reactions.

Useful auxiliary quantities

Two useful quantities associated with linear programming are the shadow prices and the reduced costs. For each linear programming problem defined by eqns (3–5), the vector of shadow prices, $\boldsymbol{w}$, is defined according to the following two equations:

$$\text{maximize } \boldsymbol{w} \,.\, \boldsymbol{b} \tag{6}$$

$$\text{subject to } \boldsymbol{w} \,.\, \mathbf{S} \leq \boldsymbol{c}. \tag{7}$$

The shadow price is the sensitivity of the objective function with respect to each constraint, i.e.:

$$\text{shadow price} = w_i = -\frac{\partial Z}{\partial b_i}.$$

In other words, if the demand of the cell for compound i is increased by Δb_i units, then the objective value Z will decrease by $w_i \,.\, \Delta b_i$ units. Thus, the shadow price is a measure of the extent to which the cell tries to violate the constraint in order to increase or decrease the value of the objective function.

The reduced costs are defined by:

$$Z = Z_0 + \boldsymbol{r} \,.\, \boldsymbol{v}_n \tag{8}$$

$$\boldsymbol{r} = \frac{\partial Z}{\partial \boldsymbol{v}_n} \tag{9}$$

where $\boldsymbol{v}_n$ is the vector of non-basic variables (i.e. fluxes with zero values in the optimal solution) and $\boldsymbol{r}$ is the vector of reduced costs. The reduced costs can be interpreted as the sensitivity of the objective function with respect to the values of the non-basic

fluxes. Thus, if the flux through the non-basic reaction i is increased from zero to γ_i, then Z will change by $r_i \cdot \gamma_i$ units.

Advantages and drawbacks

The application of linear programming for the analysis of metabolism is useful for several reasons. First, the information that is needed, the stoichiometry of the chemical reactions, is readily available. Second, kinetic rate expressions and parameters are not needed. Third, the algorithm allows one to estimate fluxes through the many interconnected pathways in response to demands on the cell. These demands can be biosynthesis, nutrient depletion, or an oversupply of a particular nutrient. Finally, one can clearly establish the effect that a particular capacity constraint, α_i, will have on other reactions. We can identify reactions which have major effects on the distributions of fluxes and reactions which have smaller effects.

There are, however, limitations to this approach to metabolic modeling. In the calculations presented here, it was assumed that the stoichiometry of the metabolic network is fixed and well-known. The addition or removal of reactions to this network due to gene induction or repression is not taken into consideration here. The stoichiometric matrix does not explicitly account for thermodynamic constraints, since there are no concentration variables. Consequently, the fluxes that are calculated may not be achievable *in vivo*. Coarse thermodynamic information can be incorporated by way of distinguishing between reversible and nearly irreversible reactions in the stoichiometric matrix. The use of linear programming necessitates the assumption that the cell tries to behave in an optimum manner with respect to some criterion. We do not prove this statement, but by comparing calculated results with experimental data, we obtain evidence that the cell does appear to operate according to particular objectives. Additionally, we can determine how the cell would behave if its metabolism was governed by these objectives. Finally, there are other constraints on the cell that were not taken into account in this network, such as transcription and translation rates, DNA replication, transport limitations, and response to hormones.

System Description

Having described the problem formulation, we now specify the various quantities that appear in eqn (4). The structure of the metabolic network, and values for the biosynthetic fluxes, were obtained using information about mammalian cells in general. The hybridoma cell line 167.4G5.3 was used as a test case in the material presented here, due to the wealth of data available on this cell line (Ozturk & Palsson, 1990). The major pathways which describe intermediary metabolism are shown in Figs 1 and 2. Wherever possible, the enzymatic reactions of pathways that are nearly linear were lumped into one reaction, with the stoichiometry shown for the overall reaction. From this network one can specify the stoichiometric matrix, shown in Table 1. The elements of the vector $\boldsymbol{b}$ that are the biosynthetic demands placed on intermediary metabolism are estimated in the following paragraphs.

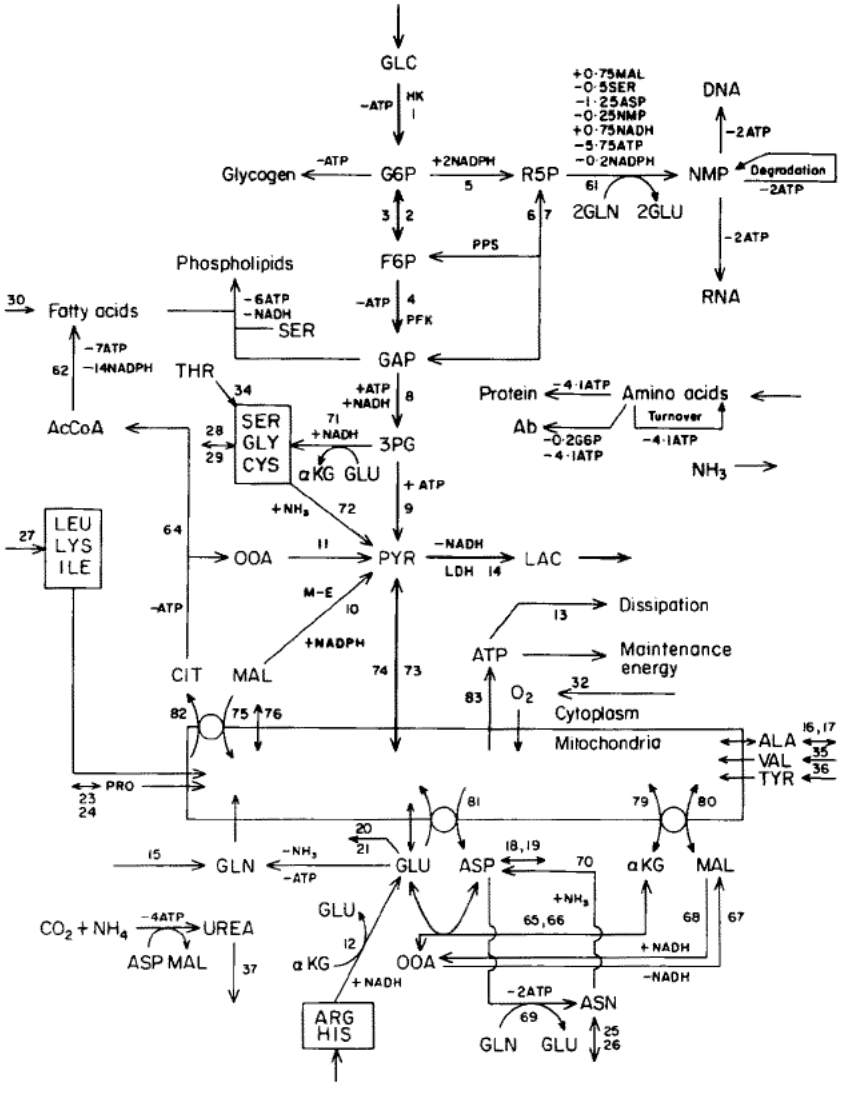

FIG. 1. Reaction pathways in the cytoplasm. Each compound is assumed to exist in a single cytoplasmic and/or mitochondrial pool, although some compounds (e.g. malate) are shown more than once in the cytoplasmic compartment for clarity. The cytoplasmic and mitochondrial pools are treated separately unless a particular mitochondrial transporter is known to exist. Abbreviations used here and in Fig. 2 are: Ab: antibody; AcCoA: acetyl CoA; ADP: adenosine diphosphate; ALA-TA: alanine-transaminase; ASP-TA: aspartate transaminase; αKG: α-ketoglutarate; αKG-DH: α-ketoglutarate dehydrogenase; ATP: adenosine triphosphate; CIT: citrate; DNA: deoxyribonucleic acid; F6P: fructose-6-phosphate; GLC: glucose; GAP: glyceraldehyde-3-phosphate; G6P: glucose-6-phosphate; GLU-DH: glutamate dehydrogenase; HK: hexokinase; LAC: lactate; LDH: lactate dehydrogenase; MAL: malate; M-E: malic enzyme; NADH: nicotinamide adenine dinucleotide; NADPH: nicotinamide adenine dinucleotide phosphate; NMP: nucleotide monophosphate; OOA: oxaloacetate; PFK: phosphofructokinase; pentose phosphate shunt; PYR: pyruvate; PDH: pyruvate dehydrogenase; RNA: ribonucleic acid; TCA: tricarboxylic acid; 3PG: 3-phosphoglycerate. The reaction numbers correspond to those given in Table 1.

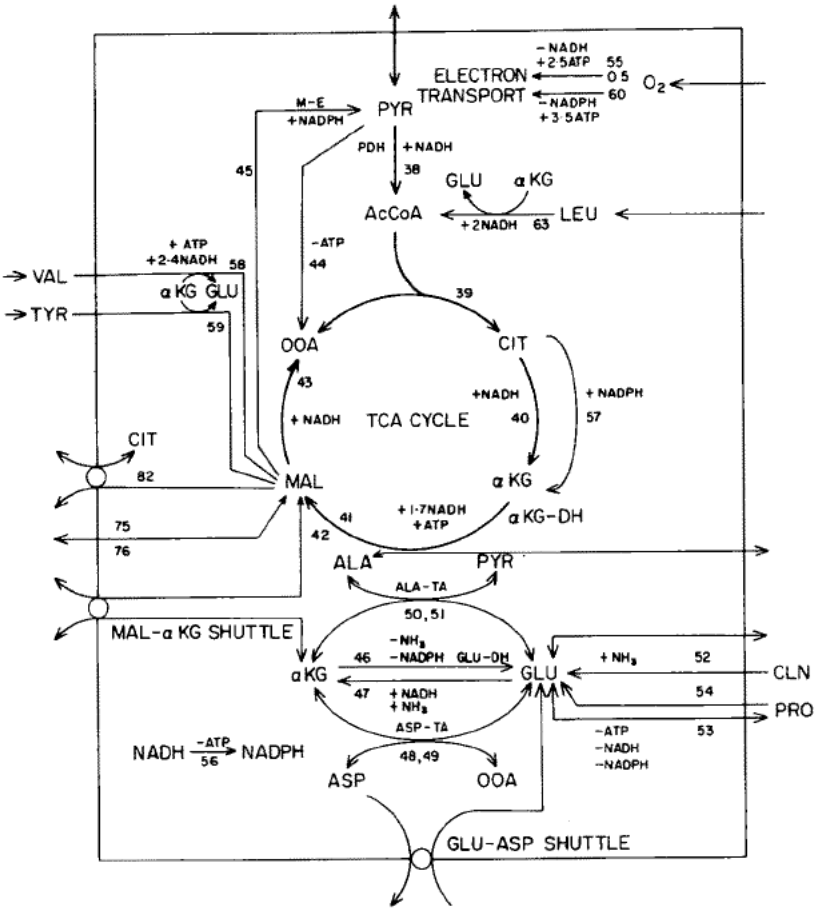

FIG. 2. Reaction pathways in the mitochondria. Abbreviations are given in Fig. 1.

Cell composition

The dry mass of the average mammalian cell is 60% protein, 4·5% nucleotides (including RNA and DNA), 16·7% lipids, 6·7% polysaccharides, and the remaining are small metabolites and ions (Alberts *et al.*, 1983). These four groups of macromolecules were taken to be representative of the cell's composition. The network was therefore constructed of the biosynthetic pathways leading to these four components, and the metabolic pathways needed to supply energy and intermediates for biosynthesis and maintenance requirements.

The amount of each compound x_i per cell was calculated according to the following general equation:

$$[x_i] = \%\text{wet wt } x_i \cdot \frac{1}{\text{MW of } x_i} \cdot \frac{1{\cdot}05 \text{ g wet wt}}{10^{12}\ \mu\text{m}^3} \cdot \frac{\text{volume}}{\text{cell}}.$$

The value of each biosynthetic flux is given by:

$$b_i = \mu \, . \, [x_i]$$

where μ is the specific growth rate. The concentration and biosynthetic flux for each major component of the cell are shown in Table 2, assuming a cell diameter of 12 μm and a doubling time of 25 hr. The details of each calculation are given in the following paragraphs.

Protein synthesis

The rate of protein synthesis needed for cell growth is shown in Table 2. Protein biosynthesis was represented by the polymerization of amino acids into protein. The cost per amino acid polymerized in eukaryotic systems is 4·1 ATP; two ATP are needed for charging the tRNA with the amino acid, and two for the elongation step on the ribosome. The 0·1 ATP is the extra cost of proofreading to ensure accuracy, which has been estimated for bacterial systems (Ingraham *et al.*, 1983). Protein turns over continuously, and the protein degradation rate was calculated from:

$$v_{deg} = k_{prt} \, . \, [\text{protein}]$$

where $k_{prt} = 0{\cdot}01 \text{ hr}^{-1}$ (Eagle & Levintow, 1965) and [protein] is given in Table 2. The degradation of protein is accomplished by two mechanisms: ATP-independent degradation by lysosomal enzymes or degradation by the ATP-dependent ubiquitin system. However, the ATP cost for degradation by the ubiquitin system is very small† compared to the total ATP cost for biosynthesis, and thus the ATP cost of degradation was neglected. The amino acid units then join the pool of amino acids in the cytoplasm, to be used in protein synthesis again.

Amino acid synthesis

The amino acids were divided into two groups: essential and non-essential. The biosynthetic pathways for the essential amino acids were not included in the network. Some of these, such as the aromatic amino acids tryptophan and phenylalanine, as well as methionine, are usually consumed in low amounts just fulfilling protein biosynthetic demands (Ozturk & Palsson, 1990; Ozturk & Palsson, 1991). These essential amino acids were lumped together under the general designation of "amino acids" (AA), and were assumed to be used only for protein synthesis, so that their catabolic pathways were not included in the network. The remaining amino acids were grouped into clusters of one, two or three amino acids, according to a common biosynthetic or catabolic route (Table 3). For example, arginine and histidine have similar catabolic routes, and both are converted to glutamate. Since arginine tends to dominate histidine in terms of media concentration and also consumption rates,

† In the ubiquitin system for protein degradation, ubiquitin is attached to the protein to be degraded with a cost of two ATPs, and several ubiquitin polypeptides may attach to a single protein. The degradation rate is about 15 nmol amino acids/10^6 cells hr^{-1}, and assuming an average size of protein of about 300 amino acids, with ten ubiquitin molecules bound per protein, and 100% of the protein degraded *via* this mechanism, then the total ATP cost for degradation is 1·0 nmol ATP/10^6 cells hr^{-1}. This value is very small compared to the total ATP demand for biosynthesis, which is about 500 nmol ATP/10^6 cells hr^{-1}.

the arginine catabolic pathway was chosen to represent both arginine and histidine catabolism. Some pathways that are rarely used, such as the export of glutamine, were not included in the system.

Monoclonal antibody synthesis

The hybridoma cell line used as a test case produces antibody at a moderate rate, so that for the general calculations, the hybridoma antibody production rate, q_{Ab},

TABLE 1

The stoichiometric matrix used for the network shown in Figs 1 *and* 2. *The letter* m *appended to the compound name indicates that the compound is in the mitochondrial compartment*

1	−1	1	0	−1	0	0	0	0	0	0	0	0	0	0
0	1	−1	−1	0	0·67	−0·67	0	0	0	0	0	0	0	0
0	0	0	2	0	0·33	−0·33	−1	0	0	0	0	0	0	0
0	0	0	0	0	0	0	1	−1	0	0	0	0	0	0
0	0	0	0	1	−1	1	0	0	0	0	0	0	0	0
0	0	0	0	0	0	0	0	0	0	0	0	0	0	0
0	0	0	0	0	0	0	0	0	0	0	0	0	0	0
0	0	0	0	0	0	0	0	1	1	1	0	0	−1	0
0	0	0	0	0	0	0	0	0	0	0	0	0	0	0
0	0	0	0	0	0	0	0	0	0	0	−1	0	0	0
0	0	0	0	0	0	0	0	0	−1	0	0	0	0	0
0	0	0	0	0	0	0	0	0	0	0	0	0	0	0
0	0	0	0	0	0	0	0	0	0	−1	0	0	0	0
0	0	0	0	0	0	0	0	0	0	0	2	0	0	0
0	0	0	0	0	0	0	0	0	0	0	0	0	0	1
0	0	0	0	0	0	0	0	0	0	0	0	0	0	0
0	0	0	0	0	0	0	0	0	0	0	0	0	0	0
0	0	0	0	0	0	0	0	0	0	0	0	0	0	0
0	0	0	0	0	0	0	0	0	0	0	0	0	0	0
0	0	0	0	0	0	0	0	0	0	0	−1	0	0	0
0	0	0	0	0	0	0	0	0	0	0	0	0	0	0
0	0	0	0	0	0	0	0	0	0	0	0	0	0	0
0	0	0	0	0	0	0	0	0	0	0	0	0	0	0
0	0	0	0	0	0	0	0	0	0	0	0	0	0	0
0	0	0	0	0	0	0	0	0	0	0	0	0	0	0
0	0	0	0	0	0	0	0	0	0	0	0	0	0	0
−1	0	0	−1	0	0	0	1	1	0	0	0	−1	0	0
0	0	0	0	0	0	0	1	0	0	0	1	0	−1	0
0	0	0	0	2	0	0	0	0	1	0	0	0	0	0
0	0	0	0	0	0	0	0	0	0	0	0	0	0	0
0	0	0	0	0	0	0	0	0	0	0	0	0	0	0
0	0	0	0	0	0	0	0	0	0	0	0	0	0	0
0	0	0	0	0	0	0	0	0	0	0	0	0	0	0
0	0	0	0	0	0	0	0	0	0	0	0	0	0	0
0	0	0	0	0	0	0	0	0	0	0	0	0	0	0
0	0	0	0	0	0	0	0	0	0	0	0	0	0	0
0	0	0	0	0	0	0	0	0	0	0	0	0	0	0
0	0	0	0	0	0	0	0	0	0	0	0	0	0	0
0	0	0	0	0	0	0	0	0	0	0	0	0	0	0
0	0	0	0	0	0	0	0	0	0	0	0	0	0	0
0	0	0	0	0	0	0	0	0	0	0	0	0	0	0
0	0	0	0	0	0	0	0	0	0	0	0	0	0	0
1	2	3	4	5	6	7	8	9	10	11	12	13	14	15

was assumed to be 0·2 pg cell^{-1} hr^{-1}, which is equivalent to 1·9 nmolAA/10^6 cells hr^{-1}. The antibody contains a carbohydrate group on each of the heavy chains. Using an average carbohydrate chain structure for IgG, and the dolichol cycle for the synthesis of the initial carbohydrate chain, the energy cost is 64 ATP and the mass cost is 26 G6P per antibody molecule synthesized. (See Appendix for details).

0	0	0	0	0	0	0	0	0	0	0	0	0	G6P
0	0	0	0	0	0	0	0	0	0	0	0	0	F6P
0	0	0	0	0	0	0	0	0	0	0	0	0	DHAP
0	0	0	0	0	0	0	0	0	0	0	0	0	3PG
0	0	0	0	0	0	0	0	0	0	0	0	0	R5P
0	0	0	0	0	0	0	0	0	0	0	0	0	NMP
0	0	0	0	0	0	0	0	0	0	0	0	0	FA
0	0	0	0	0	0	0	0	0	0	0	0	0	PYR
0	0	0	0	0	0	0	0	0	0	0	0	0	ACCOA
0	0	0	0	0	0	0	0	0	0	0	0	0	αKG
0	0	0	0	0	0	0	0	0	0	0	0	0	MAL
0	0	0	0	0	0	0	0	0	0	0	0	0	CIT
0	0	0	0	0	0	0	0	0	0	0	0	0	OOA
0	0	0	0	−1	1	0	0	0	0	0	0	0	GLU
0	0	0	0	0	0	0	0	0	0	0	0	0	GLN
0	0	0	0	0	0	0	0	0	0	0	0	−1	SER
0	0	−1	1	0	0	0	0	0	0	0	0	0	ASP
−1	1	0	0	0	0	0	0	0	0	0	0	0	ALA
0	0	0	0	0	0	0	0	0	0	0	1	0	LEU
0	0	0	0	0	0	1	0	0	0	0	0	0	ARG
0	0	0	0	0	0	0	−1	1	0	0	0	0	PRO
0	0	0	0	0	0	0	0	0	−1	1	0	0	ASN
0	0	0	0	0	0	0	0	0	0	0	0	0	THR
0	0	0	0	0	0	0	0	0	0	0	0	0	VAL
0	0	0	0	0	0	0	0	0	0	0	0	0	TYR
0	0	0	0	0	0	0	0	0	0	0	0	0	AA
0	0	0	0	0	0	0	0	0	0	0	0	0	ATP
0	0	0	0	0	0	0	0	0	0	0	0	0	NADH
0	0	0	0	0	0	0	0	0	0	0	0	0	NADPH
0	0	0	0	0	0	0	0	0	0	0	0	0	AMM
0	0	0	0	0	0	0	0	0	0	0	0	0	OXY
0	0	0	0	0	0	0	0	0	0	0	0	0	PYRM
0	0	0	0	0	0	0	0	0	0	0	0	0	ACCOA
0	0	0	0	0	0	0	0	0	0	0	0	0	CITM
0	0	0	0	0	0	0	0	0	0	0	0	0	αKGM
0	0	0	0	0	0	0	0	0	0	0	0	0	MALM
0	0	0	0	0	0	0	0	0	0	0	0	0	OOAM
0	0	0	0	0	0	0	0	0	0	0	0	0	ASPM
0	0	0	0	0	0	0	0	0	0	0	0	0	GLUM
0	0	0	0	0	0	0	0	0	0	0	0	0	NADHM
0	0	0	0	0	0	0	0	0	0	0	0	0	NADPH
0	0	0	0	0	0	0	0	0	0	0	0	0	ATPM
16	17	18	19	20	21	22	23	24	25	26	27	28	Flux

Nucleotide synthesis

Nucleotide-monophosphate (NMP) biosynthesis was represented by the *de novo* pathway. Because ribonucleotide and deoxyribonucleotide synthetic pathways are similar, these were combined into one representative pathway. The pathway leading to the synthesis of the nucleotide monophosphates, which must be phosphorylated to triphosphates before polymerization occurs, is shown in Fig. 1.

The rate of RNA and DNA synthesis needed for growth is given in Table 2. The actual rate of RNA polymerization was calculated to be much higher than that

TABLE 1—continued

0	0	0	0	0	0	0	0	0	0	0	0	0	0	0
0	0	0	0	0	0	0	0	0	0	0	0	0	0	0
0	0	0	0	0	0	0	0	0	0	0	0	0	0	0
0	0	0	0	0	0	0	0	0	0	0	0	0	0	0
0	0	0	0	0	0	0	0	0	0	0	0	0	0	0
0	0	0	0	0	0	0	0	0	0	0	0	0	0	0
0	1	0	0	0	0	0	0	0	0	0	0	0	0	0
0	0	0	0	0	0	0	0	0	0	0	0	0	0	0
0	0	0	0	0	0	0	0	0	0	0	0	0	0	0
0	0	0	0	0	0	0	0	0	0	0	0	0	0	0
0	0	0	0	0	0	0	0	1	0	0	0	0	0	0
0	0	0	0	0	0	0	0	0	0	0	0	0	0	0
0	0	0	0	0	0	0	0	0	0	0	0	0	0	0
0	0	0	0	0	0	0	0	0	0	0	0	0	0	0
0	0	0	0	0	0	0	0	0	0	0	0	0	0	0
1	0	0	0	0	0	0	0	0	0	0	0	0	0	0
0	0	0	0	0	0	0	0	−1	0	0	0	0	0	0
0	0	0	0	0	0	0	0	0	0	0	0	0	0	0
0	0	0	0	0	0	0	0	0	0	0	0	0	0	0
0	0	0	0	0	0	0	0	0	0	0	0	0	0	0
0	0	0	0	0	0	0	0	0	0	0	0	0	0	0
0	0	0	0	0	0	0	0	0	0	0	0	0	0	0
0	0	0	0	0	1	0	0	0	0	0	0	0	0	0
0	0	0	0	0	0	1	0	0	0	0	0	0	0	0
0	0	0	0	0	0	0	1	0	0	0	0	0	0	0
0	0	0	0	1	0	0	0	0	0	0	0	0	0	0
0	0	0	0	0	0	0	0	−4	0	0	0	0	0	0
0	0	0	0	0	0	0	0	0	0	0	0	0	0	0
0	0	0	0	0	0	0	0	0	0	0	0	0	0	0
0	0	−1	0	0	0	0	0	−1	0	0	0	0	0	0
0	0	0	1	0	0	0	0	0	0	0	0	0	0	0
0	0	0	0	0	0	0	0	0	−1	0	0	0	0	0
0	0	0	0	0	0	0	0	0	1	−1	0	0	0	0
0	0	0	0	0	0	0	0	0	0	1	−1	0	0	0
0	0	0	0	0	0	0	0	0	0	0	1	−1	1	0
0	0	0	0	0	0	0	0	0	0	0	0	1	−1	−1
0	0	0	0	0	0	0	0	0	0	−1	0	0	0	1
0	0	0	0	0	0	0	0	0	0	0	0	0	0	0
0	0	0	0	0	0	0	0	0	0	0	0	0	0	0
0	0	0	0	0	0	0	0	0	1	0	1	1·7	−1	1
0	0	0	0	0	0	0	0	0	0	0	0	0	0	0
0	0	0	0	0	0	0	0	0	0	0	0	1	−1	0
29	30	31	32	33	34	35	36	37	38	39	40	41	42	43

needed for growth—5·8 nmol nucleotides/million cells hr^{-1}. This higher flux is due to both the large amount of RNA processing and to RNA turnover. Detailed calculations are shown in the Appendix.

Phospholipid synthesis

Phospholipids are the major lipid constituent of the mammalian cell and are synthesized from fatty acids and glycerol-3-P. The fatty acids may either to be obtained from serum in the media, or may be synthesized from acetyl-CoA in the cytoplasm.

0	0	0	0	0	0	0	0	0	0	0	0	0	G6P
0	0	0	0	0	0	0	0	0	0	0	0	0	F6P
0	0	0	0	0	0	0	0	0	0	0	0	0	DHAP
0	0	0	0	0	0	0	0	0	0	0	0	0	3PG
0	0	0	0	0	0	0	0	0	0	0	0	0	R5P
0	0	0	0	0	0	0	0	0	0	0	0	0	NMP
0	0	0	0	0	0	0	0	0	0	0	0	0	FA
0	0	0	0	0	0	0	0	0	0	0	0	0	PYR
0	0	0	0	0	0	0	0	0	0	0	0	0	ACCOA
0	0	0	0	0	0	0	0	0	0	0	0	0	αKG
0	0	0	0	0	0	0	0	0	0	0	0	0	MAL
0	0	0	0	0	0	0	0	0	0	0	0	0	CIT
0	0	0	0	0	0	0	0	0	0	0	0	0	OOA
0	0	0	0	0	0	0	0	0	0	0	0	0	GLU
0	0	0	0	0	0	0	0	−1	0	0	0	0	GLN
0	0	0	0	0	0	0	0	0	0	0	0	0	SER
0	0	0	0	0	0	0	0	0	0	0	0	0	ASP
0	0	0	0	0	0	1	−1	0	0	0	0	0	ALA
0	0	0	0	0	0	0	0	0	0	0	0	0	LEU
0	0	0	0	0	0	0	0	0	0	0	0	0	ARG
0	0	0	0	0	0	0	0	0	1	−1	0	0	PRO
0	0	0	0	0	0	0	0	0	0	0	0	0	ASN
0	0	0	0	0	0	0	0	0	0	0	0	0	THR
0	0	0	0	0	0	0	0	0	0	0	0	0	VAL
0	0	0	0	0	0	0	0	0	0	0	0	0	TYR
0	0	0	0	0	0	0	0	0	0	0	0	0	AA
0	0	0	0	0	0	0	0	0	0	0	0	0	ATP
0	0	0	0	0	0	0	0	0	0	0	0	0	NADH
0	0	0	0	0	0	0	0	0	0	0	0	0	NADPH
0	0	1	−1	0	0	0	0	1	0	0	0	0	AMM
0	0	0	0	0	0	0	0	0	0	0	−0·5	0	OXY
−1	1	0	0	0	0	−1	1	0	0	0	0	0	PYRM
0	0	0	0	0	0	0	0	0	0	0	0	0	ACCOAM
0	0	0	0	0	0	0	0	0	0	0	0	0	CITM
0	0	1	·	1	−1	1	−1	0	0	0	0	0	αKGM
0	−1	0	0	0	0	0	0	0	0	0	0	0	MALM
1	0	0	0	−1	1	0	0	0	0	0	0	0	OOAM
0	0	0	0	1	−1	0	0	0	0	0	0	0	ASPM
0	0	−1	1	−1	1	−1	1	1	−1	1	0	0	GLUM
0	0	1	0	0	0	0	0	0	−1	1	−1	−1	NADHM
0	1	0	−1	0	0	0	0	0	−1	0	0	1	NADPH
−1	0	0	0	0	0	0	0	0	−1	0	2·5	−1	ATPM
44	45	46	47	48	49	50	51	52	53	54	55	56	Flux

Both of these pathways were included in the network. Serum-containing media is a rich source of lipids, and more than 90% of the cellular lipid is synthesized from lipids in the media (Bailey *et al.*, 1972).

Polysaccharide synthesis

The cell's polysaccharides are most likely in the form of glycogen. The rate of glycogen synthesis needed for growth is shown in Table 2. Glycogen catabolism is probably insignificant in proliferating cells in rich media, and was not included in the network.

TABLE 1—continued

0	0	0	0	0	0	0	0	0	0	0	0	0	0	0
0	0	0	0	0	0	0	0	0	0	0	0	0	0	0
0	0	0	0	0	0	0	0	0	0	0	0	0	0	0
0	0	0	0	0	0	0	0	0	0	0	0	0	0	−1
0	0	0	0	−1	0	0	0	0	0	0	0	0	0	0
0	0	0	0	0·75	0	0	0	0	0	0	0	0	0	0
0	0	0	0	0	1	0	0	0	0	0	0	0	0	0
0	0	0	0	0	0	0	0	0	0	0	0	0	0	0
0	0	0	0	0	−8	0	1	0	0	0	0	0	0	0
0	0	0	0	0	0	0	0	−1	1	0	0	0	0	1
0	0	0	0	0·75	0	0	0	0	0	1	−1	0	0	0
0	0	0	0	0	0	0	−1	0	0	0	0	0	0	0
0	0	0	0	0	0	0	1	1	−1	−1	1	0	0	0
0	0	0	0	2	0	0	0	1	−1	0	0	1	0	−1
0	0	0	0	−2	0	0	0	0	0	0	0	−1	0	0
0	0	0	0	−0·5	0	0	0	0	0	0	0	0	0	1
0	0	0	0	−1·25	0	0	0	−1	1	0	0	−1	1	0
0	0	0	0	0	0	0	0	0	0	0	0	0	0	0
0	0	0	0	0	0	−1	0	0	0	0	0	0	0	0
0	0	0	0	0	0	0	0	0	0	0	0	0	0	0
0	0	0	0	0	0	0	0	0	0	0	0	0	0	0
0	0	0	0	0	0	0	0	0	0	0	0	1	−1	0
0	0	0	0	0	0	0	0	0	0	0	0	0	0	0
0	−1	0	0	0	0	0	0	0	0	0	0	0	0	0
0	0	−1	0	0	0	0	0	0	0	0	0	0	0	0
0	0	0	0	0	0	0	0	0	0	0	0	0	0	0
0	0	0	0	−5·75	−7	0	−1	0	0	0	0	−2	0	0
0	0	0	0	0·75	0	0	0	0	0	−1	1	0	0	1
0	0	0	0	−0·2	−14	0	0	0	0	0	0	0	0	0
0	0	0	0	0	0	0	0	0	0	0	0	0	1	0
0	0	0	−0·5	0	0	0	0	0	0	0	0	0	0	0
0	0	0	0	0	0	0	0	0	0	0	0	0	0	0
0	0	0	0	0	0	1	0	0	0	0	0	0	0	0
−1	0	0	0	0	0	0	0	0	0	0	0	0	0	0
1	−1	−1	0	0	0	−1	0	0	0	0	0	0	0	0
0	1	1	0	0	0	0	0	0	0	0	0	0	0	0
0	0	0	0	0	0	0	0	0	0	0	0	0	0	0
0	0	0	0	0	0	0	0	0	0	0	0	0	0	0
0	1	1	0	0	0	1	0	0	0	0	0	0	0	0
0	2·4	0	0	0	0	2	0	0	0	0	0	0	0	0
1	0	0	−1	0	0	0	0	0	0	0	0	0	0	0
0	1	0	3·5	0	0	0	0	0	0	0	0	0	0	0
57	58	59	60	61	62	63	64	65	66	67	68	69	70	71

Energy metabolism

In addition to the biosynthetic pathways for most of the cell components, and catabolic pathways for the amino acids, the major pathways for mass, energy, and redox metabolism were included in the network. These pathways are: glycolysis, PPS, and the TCA cycle. Pathways that occur only in certain specialized cells were not included, and thus the results presented here are not applicable to those cell types that contain these reactions. Fatty acid oxidation was not included because it has been shown that this pathway contributes less than 10% of the total energy needs of

0	0	0	0	0	0	0	0	0	0	0	0	G6P
0	0	0	0	0	0	0	0	0	0	0	0	F6P
0	0	0	0	0	0	0	0	0	0	0	0	DHAP
0	0	0	0	0	0	0	0	0	0	0	0	3PG
0	0	0	0	0	0	0	0	0	0	0	0	R5P
0	0	0	0	0	0	0	0	0	0	0	0	NMP
0	0	0	0	0	0	0	0	0	0	0	0	FA
1	−1	1	0	0	0	0	0	0	0	0	0	PYR
0	0	0	0	0	0	0	0	0	0	0	0	ACCOA
0	0	0	0	0	0	0	1	−1	0	0	0	αKG
0	0	0	−1	1	0	0	−1	1	0	−1	0	MAL
0	0	0	0	0	0	0	0	0	0	1	0	CIT
0	0	0	0	0	0	0	0	0	0	0	0	OOA
0	0	0	0	0	−1	1	0	0	−1	0	0	GLU
0	0	0	0	0	0	0	0	0	0	0	0	GLN
−1	0	0	0	0	0	0	0	0	0	0	0	SER
0	0	0	0	0	0	0	0	0	1	0	0	ASP
0	0	0	0	0	0	0	0	0	0	0	0	ALA
0	0	0	0	0	0	0	0	0	0	0	0	LEU
0	0	0	0	0	0	0	0	0	0	0	0	ARG
0	0	0	0	0	0	0	0	0	0	0	0	PRO
0	0	0	0	0	0	0	0	0	0	0	0	ASN
0	0	0	0	0	0	0	0	0	0	0	0	THR
0	0	0	0	0	0	0	0	0	0	0	0	VAL
0	0	0	0	0	0	0	0	0	0	0	0	TYR
0	0	0	0	0	0	0	0	0	0	0	0	AA
0	0	0	0	0	0	0	0	0	0	0	1	ATP
0	0	0	0	0	0	0	0	0	0	0	0	NADH
0	0	0	0	0	0	0	0	0	0	0	0	NADPH
1	0	0	0	0	0	0	0	0	0	0	0	AMM
0	0	0	0	0	0	0	0	0	0	0	0	OXY
0	1	−1	0	0	0	0	0	0	0	0	0	PYRM
0	0	0	0	0	0	0	0	0	0	0	0	ACCOAM
0	0	0	0	0	0	0	0	0	0	−1	0	CITM
0	0	0	0	0	0	0	−1	1	0	0	0	αKGM
0	0	0	1	−1	0	0	1	−1	0	1	0	MALM
0	0	0	0	0	0	0	0	0	0	0	0	OOAM
0	0	0	0	0	0	0	0	0	−1	0	0	ASPM
0	0	0	0	0	1	−1	0	0	1	0	0	GLUM
0	0	0	0	0	0	0	0	0	0	0	0	NADHM
0	0	0	0	0	0	0	0	0	0	0	0	NADPH
0	0	0	0	0	0	0	0	0	0	0	−1	ATPM
72	73	74	75	76	77	78	79	80	81	82	83	Flux

TABLE 2

Calculation of the biosynthetic rates in the cell, using a cell diameter equal to 12 μm and doubling time equal to 25 hr

Macromolecule	Amount cell^{-1} (g/100 g wet wt) (Alberts *et al.*, 1983)	Molecular weight	Corresponding monomer concentration (nmol/10^6 cells)	Corresponding monomer flux (nmol /10^6 cells hr^{-1})
Protein	18	108 g AA mol^{-1}	1584	43·6
RNA	1·1	358 g NMP mol^{-1}	29·2	0·8
DNA	0·25	342 g NMP mol^{-1}	6·9	0·2
Phospholipid	5	769 g PL mol^{-1}	61·8	1·7
Polysaccharide	2	162 g PS mol^{-1}	117·3	3·2

transformed cells cultivated *in vitro* (Eigenbrodt *et al.*, 1985). The reactions of the electron transport chain were represented by one overall reaction, with a P/O ratio of 2·5 (Beavis & Lehninger, 1986; Lemasters, 1984) for NADH and 3·5 for NADPH.

An ATP mass balance forces the energy metabolism pathways to provide enough energy to meet the biosynthetic demands. However, not all the energy demands of the cell can be accounted for by biosynthesis, and the remaining energy needs are put in the category of "maintenance" energy. This maintenance term includes energy costs for transport, maintenance of gradients, metabolic reactions that have not been included, and maintenance of the cell structure. The maintenance ATP requirement,

TABLE 3

Groupings of amino acids

Amino acid group name	Amino acid	Essential (E) or non-essential (N)	Occurrence in proteins, (%) (Creighton, 1984)
ARG	Arginine	E	4·7
	Histidine	E	2·1
ASN	Asparagine	N	4·4
ASP	Aspartate	N	5·5
ALA	Alanine	E	9·0
GLN	Glutamine	N	3·9
GLU	Glutamate	N	4·6
LEU	Leucine	E	7·5
	Lysine	E	7·0
	Isoleucine	E	4·6
PRO	Proline	N	4·6
SER	Serine	N	7·1
	Glycine	N	7·5
	Cysteine	N	2·8
THR	Threonine	E	6·0
TYR	Tyrosine	N	3·5
VAL	Valine	E	6·9
AA	Methionine	E	1·7
	Phenylalanine	E	3·5
	Tryptophan	E	1·1

m, is defined by (Pirt, 1982):

$$q_{ATP} = \frac{\mu}{Y_{ATP/cell}} + m \tag{10}$$

where $Y_{ATP/cell}$ is the moles of ATP produced per mass of cells. Estimates for m have been obtained from the following sources (in nmol ATP/million cells hr^{-1}): 510 in fibroblasts (Fleischaker, 1986), 600 in hybridomas (Miller *et al.*, 1986), and 515 in mouse LS cells (after being normalized to the hybridoma volume) (Kilburn *et al.*, 1969). The value of 600 was chosen for this network.

Results and Discussion

We will now analyze cell metabolism using only the information inherent in the stoichiometric matrix. We have addressed four topics: (1) influence of the choice of objective function on the flux distribution; (2) comparison of amino acids as nutrients; (3) study of glucose as nutrient; (4) interaction of glucose and glutamine as nutrients.

(A) EFFECT OF OBJECTIVE FUNCTION

We first examined how the assumed objective influences the way the cell makes use of resources. For a unicellular organism, the survivability of the cell depends on the cell's ability to maximize its growth rate in various environments. The objective of individual cells in a multicellular organism is not as clear. For example, a mammalian cell may secrete a product or perform some function as part of its role in the body, as well as grow efficiently and in a controlled manner. Such a cell most likely has more than one objective and these objectives may change with time and situation. However, the optimal use of resources such as mass, ATP, and redox potential is logical for the organism's survivability. An examination of how metabolically reasonable objectives influence the flux distribution gives insight into what may be appropriate objectives for the cell.

In these calculations no capacity restrictions were placed on any of the reactions in the network, in order to allow the stoichiometric network to have maximum flexibility. The doubling time was fixed at 25 hr and the cell diameter was set to 12 μm, which sets all the biosynthetic requirements, and the maintenance demand was set to 600 nmol ATP/10^6 cells hr^{-1}. These values are representative for tumor cell growth *in vitro* (Fleischaker, 1986; Miller *et al.*, 1986; Kilburn *et al.*, 1969).

We calculated the expected behavior of the cell, assuming that the cell distributes its mass and energy resources according to certain criteria based on stoichiometry. The three objective functions examined were: (1) optimize energy efficiency by minimizing ATP production, (2) optimize use of substrates by minimizing total nutrient uptake, and (3) optimize with respect to redox metabolism by minimizing NADH production. The mathematical form of the objective functions are shown in Table 4, and results from these calculations are summarized in Table 5 and discussed below.

TABLE 4

Mathematical form of the objective functions used in this paper, where v_i *is the flux through reaction* i

Objective function	
Minimize ATP production	$v_8 + v_9 + v_{41} + 2{\cdot}5v_{55} + v_{58} + 3{\cdot}5v_{60}$
Minimize moles nutrient uptake	$v_1 + v_{15} + v_{17} + v_{19} + v_{21} + v_{22} + v_{24} + v_{26} + v_{27} + v_{29} + v_{30} + v_{33} + v_{34} + v_{35} + v_{36}$
Minimize mass nutrient uptake	$180v_1 + 146v_{15} + 89v_{17} + 132v_{19} + 147v_{21} + 165v_{22} + 115v_{24} + 132v_{26} + 136v_{27} + 100v_{29} + 255v_{30} + 120v_{33} + 119v_{34} + 117v_{35} + 181v_{36}$
Minimize NADH production	$2v_5 + v_8 + v_{10} + v_{12} + v_{38} + v_{40} + 1{\cdot}7v_{41} + v_{43} + v_{45} + v_{46} + v_{54} + v_{57} + 2{\cdot}4v_{58} + 0{\cdot}75v_{61} + 2v_{63} + v_{68} + v_{71}$

Minimize ATP production

The objective function of minimizing ATP production represents the concept that the cell strives to operate in terms of energy efficiency. The use of this objective function assumes that the cell consumes nutrients and distributes its mass and energy in such a way as to produce only as much energy as is needed for cell growth.

When ATP production was minimized, the amino acids were preferred over glucose as an energy source. The glucose consumption rate (q_{GLC}) of 5 nmol/10^6 cells hr^{-1} was used completely for biosynthesis of lipids, polysaccharides, and nucleotides. Growth on any of the amino acids gave the same ATP production rate, but growth on glucose caused the ATP production to increase. The oxygen consumption ranged from 150–164 nmol/10^6 cells hr^{-1}, falling within the range reported (Thomas, 1986) for animal cells. The yield coefficient, $Y_{c/s}$ (defined as mass of cells/mass of substrate consumed), ranged from 0·48 for growth on serine, to 0·61 for growth on proline, which are comparable to the $Y_{c/s}=0{\cdot}5$ for bacteria grown aerobically on glucose (Ingraham *et al.*, 1983). The ATP production rate of 891 nmol/10^6 cells hr^{-1} was the minimum amount of ATP necessary for cell growth and maintenance. This ATP production rate is similar to that reported for hybridoma cells (Miller *et al.*, 1988*b*; Ozturk & Palsson, 1991).

However, when ATP usage was removed from both the hexokinase and phosphofructokinase reactions, we find that the amino acids were no longer the preferred

TABLE 5

Summary of results obtained using three objective functions, with no constraints on the system

Objective function	$Y_{c/s}$ g dry wt cells g^{-1} nutrients	q_{O_2}	q_{ATP}	$q_{NAD(P)H}$ nmol/10^6 cells hr^{-1}	Major nutrients
Minimize ATP	0·48–0·61	150–164	891	300–331	Amino acids
Minimize moles nutrients	0·58	151	950	380	GLC, ARG
Minimize mass nutrients	0·64	154	905	328	PRO
Minimize NADH	0·13–0·32	127–137	891	255–277	TYR, GLN

nutrients and that glucose was consumed in large amounts (calculations not shown). The objective of minimizing ATP production is formulated such that the total flux through all reactions which produce ATP was minimized. The yield of ATP from glucose when metabolized anaerobically is two ATP/GLC, but the total flux through ATP producing reactions must be 4 units for each unit of glucose, to account for the ATP usage by hexokinase and phosphofructokinase. On the other hand, ATP is not consumed during catabolism of glutamine, so that the flux of 23 units through ATP producing reactions for each unit of glutamine catabolized (assuming complete oxidation, and a P/O ratio of 2·5) is exactly equal to the yield of ATP from glutamine. Consequently, we concluded that amino acids were the preferred nutrients because ATP was not needed to "spark" the catabolism of amino acids, as was needed for glucose.

Minimizing ATP production yields results that correspond to experimental observations to a certain extent. Glutamine has been reported to provide 30–50% of the energy for cells in culture (McKeehan, 1986), and a substantial amount of the biomass as well. According to this computation, amino acids are the preferred nutrients from an energetic standpoint.

Minimize nutrient uptake

With this objective function we assumed that the cell is able to consume a limited amount of nutrients, so that the cell must minimize its nutrient uptake rate for a specified growth rate. This objective function may be realistic during conditions of limited availability of nutrients, e.g. starvation for cells *in vivo*, and after nutrient depletion for cells cultured *in vitro*.

Glucose was preferred over all the amino acids for the production of mass and energy when the total molar uptake of nutrients was minimized. The glucose uptake rate was 32 nmol/10^6 cells hr^{-1}. Glucose oxidation in the TCA cycle generated the cell's energy, replacing amino acid oxidation from the previous simulation. Arginine was the only amino acid consumed in amounts greater (by a factor of 4·3) than that needed directly for biosynthesis.

When the total *mass* uptake of nutrients was minimized, proline was preferred over glucose as the nutrient source. The mass yield had the value of $Y_{c/s} = 0{\cdot}64$, which was therefore the maximum yield. The ATP production was 905 nmol/10^6 cells hr^{-1}, which was nearly the same as the minimizing ATP result. Proline has five carbons, vs. the six carbons of glucose, and although the ATP/carbon yield is greater for proline than glucose, the larger number of carbons in glucose causes the ATP/mol yield to be greater for glucose than proline. Consequently, glucose is preferred when moles of substrate are minimized, while proline is preferred when mass of substrate is minimized. A slight tradeoff between mass and energy efficiency was observed, since in order to reduce the molar nutrient uptake, the ATP production rate increased by 7% over the minimizing ATP production result. To reduce mass uptake, the ATP production increased by 2% over the minimizing ATP production result.

Minimize the production of redox potential

The objective of minimizing NADH production may be realistic, since it would not be beneficial for the cell to have an excess of oxidizing reactions present. The

results obtained with this objective function were significantly different from those obtained with the three objectives previously discussed. Under this objective, most of the mass and energy were supplied by tyrosine. When the catabolic pathway for tyrosine was removed from the network, the preferred nutrient was glutamine, with the excess mass secreted as alanine. The mass efficiencies for these two nutrients were low ($Y_{c/s}=0{\cdot}32$ for growth on glutamine, $Y_{c/s}=0{\cdot}13$ for growth on tyrosine), but the energy yields were identical to the minimizing ATP system. The primary energy generating reactions were catalyzed by α-ketoglutarate dehydrogenase (αKG-DH) and malic enzyme. The overall energy metabolism can be described by:

$$\mathrm{GLN} + 1{\cdot}7\mathrm{NAD}^+ + \mathrm{ADP} + \mathrm{NADP}^+ \rightarrow \mathrm{ALA} + 1{\cdot}7\mathrm{NADH} + \mathrm{ATP} + \mathrm{NADPH} + \mathrm{NH_3} + 2\mathrm{CO_2}.$$

These results are similar qualitatively to results observed in culture, i.e. large uptake of glutamine and production of alanine.

Comparison of objective functions

A comparison of the results using different objective functions is shown in Table 5. The ATP production rate is relatively constant among the different objectives, indicating that none of the objectives cause the cell to produce excess energy. Conversely, the mass yields vary considerably, by more than a factor of 4. Both redox production and oxygen uptake rate show moderate variations of 20% and 13%, respectively.

Although no single objective function gave results that completely describe the actual behavior of the hybridoma cell, certain objectives do give results characteristic of particular aspects of hybridoma cell behavior. The objective function of minimizing redox production resulted in mass yields that are low compared to those resulting from the other objective functions, and this inefficiency with respect to consumption of nutrients is an observed characteristic of the hybridoma cell and other tumor cell lines. This objective function resulted in large rates of glutamine uptake and alanine production, which are characteristic of hybridoma cell behavior. The ATP production, on the other hand, was the same as that calculated when ATP production was minimized. Minimizing redox production also causes the oxygen uptake rate to be the lowest of the objective functions. These results suggest that the objective of minimizing NADH production may be a realistic objective for the hybridoma call.

The cell appears to behave, at least partially, in order to minimize ATP production, since minimizing ATP production causes the cell to consume amino acids as the major nutrient. A similar result was obtained when mass uptake was minimized, indicating that these may be parallel objectives. The minimizing moles of nutrients objective did not mimic the key characteristic of tumor cells of a large rate of amino acid oxidation, so this is unlikely to be a realistic objective.

(B) AMINO ACIDS AS NUTRIENTS

Linear optimization provides a means for comparing the role of different nutrients, in particular the amino acids, for support of growth and metabolism. The amino

acids are all catabolized to a limited number of intermediates, which are then distributed further along catabolic and anabolic pathways for energy generation and biosynthesis. The stoichiometry of these pathways determines how valuable a compound is as a nitrogen, carbon, and energy source. The value of the amino acids for growth is dependent on the point at which the compound enters the intermediary metabolism, the stoichiometry of the reaction leading to this point, as well as the transporter and enzyme kinetics involved in the processing of the amino acid.

By calculating the maximum growth rate and shadow price for growth on a single amino acid, we examined the compound's ability to satisfy carbon, nitrogen, and energy demands simultaneously. We can then identify the amino acids that are best able to meet all the requirements for growth by their ability to provide the highest theoretical growth rate.

In the calculations in this subsection, the uptake rates of the non-essential amino acids and the catabolic pathways of the essential amino acids were removed from the stoichiometric matrix. Glucose was allowed to be consumed in quantities sufficient for polysaccharide, lipid, and nucleotide synthesis, but could not be catabolized further than these pathways. The uptake rate of each non-essential amino acid was individually assigned the value of 100 nmol/10^6 cells hr^{-1}, only as a reference point, and the maximum growth rate then calculated. To calculate the growth rate on the essential amino acids, the catabolic pathway for each amino acid was individually assigned the value of 100 nmol/10^6 cells hr^{-1}. This setup insures that the load for essential amino acids did not affect the growth calculations. This problem formulation is essentially the same as if the growth rate was fixed, and the uptake rate of each individual amino acid was minimized.

The amino acids with catabolic pathways that lead directly to glutamate—arginine, proline, glutamine, and glutamate—provided the highest growth rate (Table 6). Valine also yielded a high growth rate, although it was not catabolized directly to

TABLE 6

Growth yields with amino acids as primary nutrients. The second column shows the maximum growth rate obtained for growth on glucose and the single amino acid listed in column 1. *Growth rates were normalized to the average growth rate of* 0·0275 hr^{-1}, *or doubling time of* 25 *hr. The ATP and cell mass yields were calculated by setting the growth rate equal to* 0·0275 hr^{-1}, *and minimizing the rate of nutrient uptake*

Amino acid	Growth rate	ATP/C	$C_{cell\ mass}/C$
Alanine	1·71	3·9	0·28
Arginine	4·25	3·3	0·24
Asparagine	1·75	2·9	0·21
Aspartate	1·73	2·9	0·21
Glutamate	3·33	3·6	0·25
Glutamine	3·37	3·6	0·26
Proline	3·86	4·0	0·28
Serine	1·22	2·9	0·21
Tyrosine	2·36	1·5	0·11
Valine	3·65	3·6	0·26

glutamate, because of its high energy value in terms of NAD^+ reduction and ATP formation.

The result that the glutamine growth yield was slightly higher than the glutamate growth yield may be due either to the cost of one ATP to synthesize glutamine from glutamate, or due to the extra amino group carried by glutamine. From Table 7, we see that the shadow price for ammonia was always zero, indicating that the growth rate was insensitive to the amount of free ammonia. Consequently, the advantage to the cell from consuming glutamine rather than glutamate must be due to the difference in ATP cost rather than amino group content.

The amino acids tyrosine, alanine, aspartate, and asparagine are catabolized *via* transamination to glutamate. The carbon skeleton of alanine and aspartate, which require transamination, end up in TCA intermediates with less energy value than α-ketoglutarate, and consequently resulted in lower growth rates. Growth on serine depends on the cell's ability to capture free ammonia in the αKG-DH reaction. Since the catabolic product from serine is pyruvate, which has only three carbon atoms, the yield on serine was relatively low.

The shadow prices were helpful in identifying the features of the network that were the limiting factors for cell growth. As shown in Table 7, the shadow prices of both amino acids and TCA intermediates were non-zero for growth on all nutrients, while free ammonia had a shadow price of zero. This result indicated that the cells were limited for carbon, and not amino groups, for growth. It is unlikely that energy

TABLE 7

Shadow prices for growth on a single amino acid and glucose

Nutrient: \ Shadow price:	GLU	GLN	ASP	ALA	ATP	NADH
Alanine	0·046	0·048	0·032	0·030	0·0018	0·0046
Arginine	0·046	0·048	0·032	0·030	0·0018	0·0046
Asparagine	0·047	0·049	0·031	0·031	0·0019	0·0066
Aspartate	0·047	0·048	0·030	0·030	0·0019	0·0065
Glutamate	0·046	0·048	0·032	0·030	0·0019	0·0046
Glutamine	0·047	0·047	0·032	0·030	0·0019	0·0047
Proline	0·047	0·049	0·032	0·031	0·0019	0·0047
Serine	0·047	0·048	0·033	0·031	0·0018	0·0045
Tyrosine	0·046	0·048	0·032	0·030	0·0018	0·0046
Valine	0·046	0·048	0·032	0·030	0·0018	0·0046

Nutrient: \ Shadow price:	NADPHm	NH_3	CIT	αKG	MAL	OOA	PYR
Alanine	0·0065	0·0	0·048	0·042	0·032	0·027	0·025
Arginine	0·0065	0·0	0·048	0·042	0·032	0·027	0·025
Asparagine	0·0066	0·0	0·049	0·042	0·033	0·028	0·026
Aspartate	0·0065	0·0	0·048	0·042	0·032	0·027	0·026
Glutamate	0·0065	0·0	0·048	0·042	0·032	0·027	0·025
Glutamine	0·0065	0·0	0·049	0·042	0·032	0·028	0·026
Proline	0·0066	0·0	0·049	0·042	0·032	0·028	0·026
Serine	0·0063	0·0	0·047	0·040	0·031	0·026	0·025
Tyrosine	0·0065	0·0	0·048	0·042	0·032	0·027	0·025
Valine	0·0065	0·0	0·048	0·042	0·032	0·027	0·025

limitation was very important, since the shadow price for ATP was about 1/15 of that of the TCA intermediates. The shadow price for NADH was usually greater than that of ATP by a factor of 2·5, which resulted directly from the stoichiometry of the electron transport chain. However, for growth on asparagine and aspartate, this factor increased to 3·5, indicating that the growth rate was more sensitive to the NADH demand when the nutrients were asparagine and aspartate. This result suggested that the catabolism of aspartate yields an intermediate that is less useful in terms of NADH generation than the other amino acids.

The shadow prices of the TCA intermediates were proportional to their position in the TCA cycle. For example, the shadow price of malate was greater than oxaloacetate by 0·004 units. This value resulted because the shadow price of one NADH was 0·004, and the malate dehydrogenase reaction reduces one NAD^+. Similarly, the price of α-ketoglutarate was 0·010 units greater than malate. This difference can be accounted for by the cofactor production of 1·7 NADH, and 1 ATP (see Fig. 2): $1{\cdot}7(0{\cdot}0046) + 1(0{\cdot}0018) = 0{\cdot}010$. Consequently, the difference between α-ketoglutarate and malate was due entirely to redox potential and energy, and not to carbon content.

The yields of ATP and carbon used in biomass from each carbon atom of the amino acid were calculated by constructing the network so that only the specified amino acid was consumed, and by setting the growth rate equal to 0·0275 hr^{-1} (Table 6). The uptake rate of the amino acid was then minimized. The amount of ATP and carbon needed for a growth rate of 0·0275 hr^{-1} was calculated, and divided by the number of carbon atoms of the nutrient amino acid to give the yields. Proline and alanine were most efficient in terms of both energy and carbon yields.

In conclusion, the amino acids that are catabolized directly to glutamate, rather than through transamination, gave the greatest growth yields. However, the greatest energy and mass yields on a per carbon basis were given by proline and alanine. Additionally, the growth rate was sensitive to TCA intermediates due to their value as energy sources, rather than as carbon sources.

(C) GLUCOSE AS NUTRIENT

ATP yield from glucose

The calculated maximum yield of ATP per carbon atom in glucose is shown in Fig. 3 as a function of oxygen uptake rate. To obtain the yield for glucose, the network was modified such that amino acids could be consumed only for biosynthesis, causing glucose to be the only energy source, and the uptake rate of glucose was minimized. At near anaerobic conditions, the calculated ATP/carbon yield is nearly the same as the theoretical anaerobic yield of 0·33 ATP/carbon. The calculated maximum yield of 5·3 ATP/carbon occurred at q_{O_2} equal to 150 nmol/10^6 cells hr^{-1}, and is equal to 98% of the theoretical yield for complete oxidation of glucose (assuming $P/O = 2{\cdot}5$). As a result, only a very small percentage of glucose is consumed for biosynthesis.

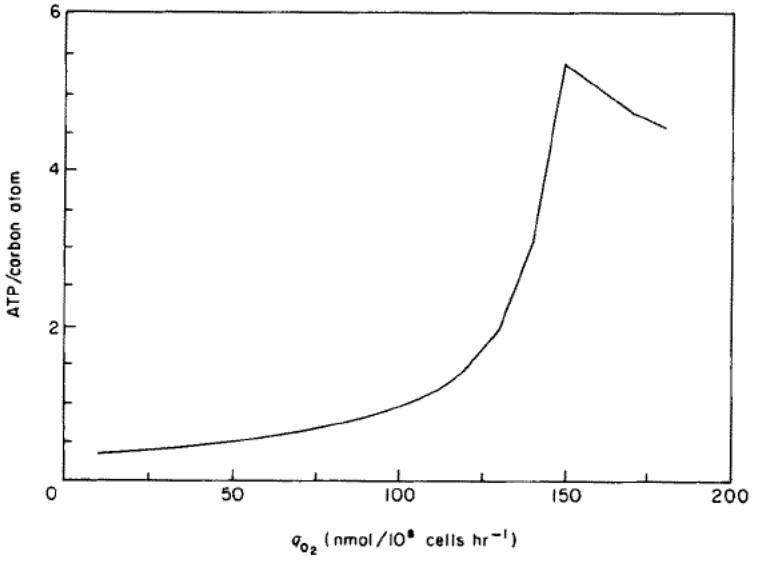

FIG. 3. Effect of oxygen uptake on the yield of ATP from glucose. The growth rate was set to 0·0275 hr^{-1}, and the uptake rate of glucose was minimized.

(D) INTERACTION OF GLUCOSE AND GLUTAMINE

Glucose and glutamine are the primary nutrients for the hybridoma cell, and their interaction occurs in the reactions involving pyruvate, the TCA cycle, and some transaminases. Linear optimization allows us to easily compare how limitations on a particular enzyme activity will affect the catabolism of these two nutrients and the cell's growth ability. In other words, we can predict how the deletion of a gene for a particular enzyme, or the inhibition of an enzyme, would affect the cell's performance, and thus identify reactions which are either required or unnecessary for cell growth. Another application of linear optimization is to predict the effect of different parameters on cell metabolism. Here we examine the effect of a capacity restriction on the malate-aspartate (MAL-ASP) shuttle on nutrient selection, and on the ratio of glucose to glutamine uptake rates that is optimal for growth.

Influence of malate-aspartate shuttle on nutrient demand

The mitochondrial membrane is impermeable to the redox equivalents produced during glycolysis; hence these must be transferred indirectly to the mitochondria *via* a shuttle mechanism. The (MAL-ASP) shuttle has been found to be the primary mechanism for shuttling redox equivalents in tumor cells (Greenhouse & Lehninger, 1976; Lopez-Alarcon *et al.*, 1979; Perez-Rodriguez *et al.*, 1987). This shuttle consists of the following reactions: GLU-ASP transporter, MAL-αKG transporter, ASP-TA in cytoplasm and mitochondria, MAL-DH in cytoplasm and mitochondria, and αKG-DH in mitochondria (see Fig. 2).

In a cell with no constraints, glucose was found to be capable of fulfilling most biosynthetic and energy demands, as long as there was some nitrogen source (see Table 5). However, a limit on the MAL-ASP shuttle reduces the amount of cytoplasmic redox equivalents that can be shuttled into the mitochondria and subsequently converted into high energy phosphate bonds. When the flux through this shuttle is constrained, the redox equivalents must be removed *via* the lactate dehydrogenase step. Pyruvate must then be secreted as lactate rather than oxidized in the TCA cycle, thus reducing the rate of glucose oxidation. Although MAL-ASP shuttle was found to operate in tumor cells (Greenhouse & Lehninger, 1976; Lopez-Alarcon *et al.*, 1979), there is some evidence that low concentrations of aspartate may limit the flux through the shuttle (Eigenbrodt *et al.*, 1985).

In the next set of simulations we examined the effect of a constraint on the MAL-ASP shuttle on nutrient selection. The objective function of minimizing nutrient consumption was used (Table 4). No capacity restrictions were placed on any of the reactions, except for the MAL-ASP shuttle.

The effect of the MAL-ASP shuttle on nutrient selection is shown in Fig. 4. As the MAL-ASP shuttle constraint was lowered, the rate of proline uptake increased, replacing glucose as the supplier of mass and ATP. Due to realistic constraints on the proline catabolic pathway, however, glutamine may be used to fulfill the energy and biosynthetic needs. These results thus agree with the suggestion (Eigenbrodt *et al.*, 1985) that limitation of the MAL-ASP shuttle activity may be one factor causing the cell's preference, as observed in culture conditions (Eigenbrodt *et al.*, 1985; Miller *et al.*, 1988*a*; Ozturk & Palsson, 1990), for glutamine as a nutrient.

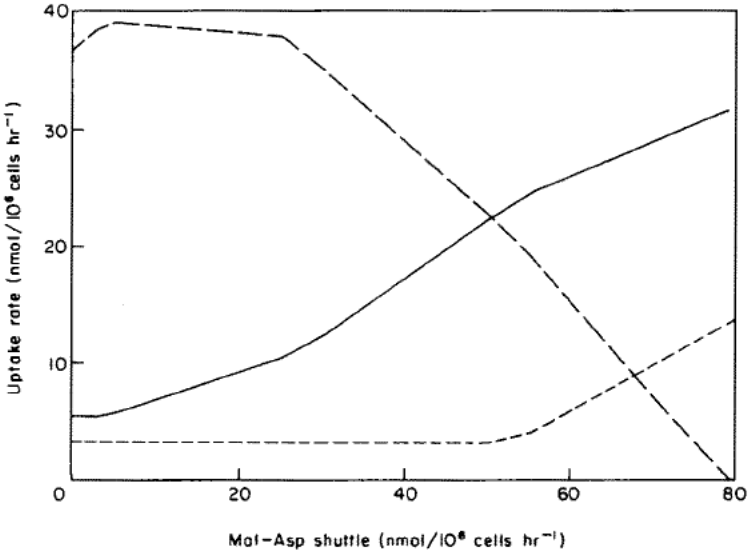

FIG. 4. Effect of maximum capacity of the malate-aspartate shuttle on choice of nutrients when nutrient uptake was minimized. (———), Glucose; (— — —), proline; (- - -), arginine.

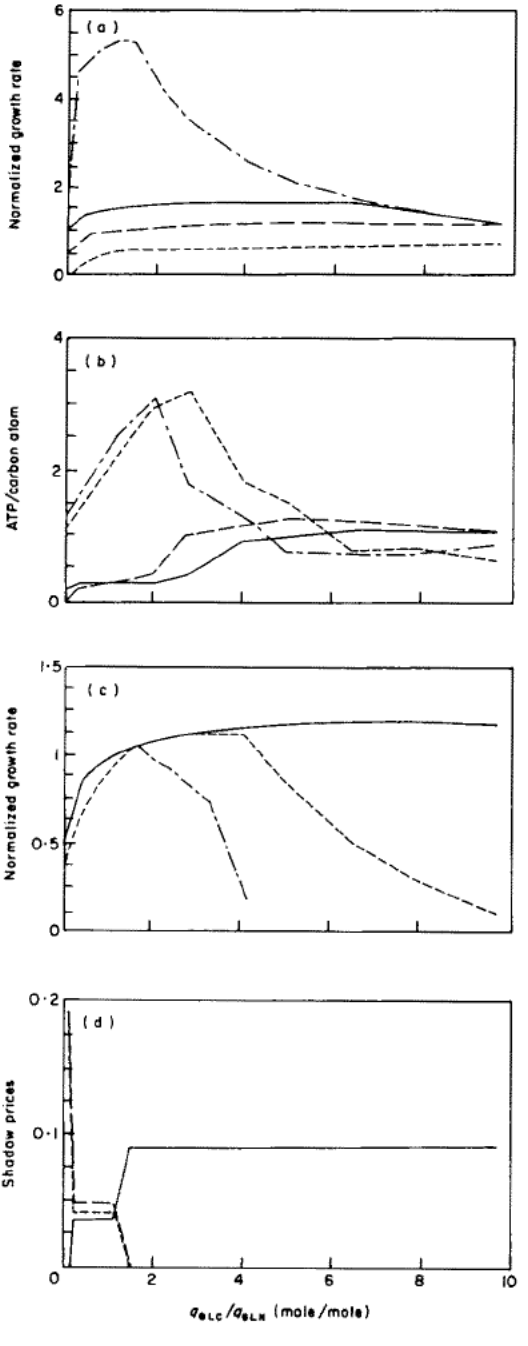
(a)
Normalized growth rate
6
4
2
0
(b)
ATP/carbon atom
4
2
0
(c)
Normalized growth rate
1·5
1
0·5
0
(d)
Shadow prices
0·2
0·1
0
2
4
6
8
10
q_{GLC}/q_{GLN} (mole/mole)

Effects of relative uptake rates of glucose to glutamine on growth rate

The cell culture media's concentrations of glucose and glutamine have been formulated, from years of testing, to give the best growth rate and cell viability. In general, the ratio of the initial molar concentration of glucose to glutamine in tissue culture media is 4–8. The ratio of q_{GLC}/q_{GLN} for hybridomas grown in continuous culture ranges from 2–8 mole/mole (Miller *et al.*, 1988*a*; Ozturk & Palsson, 1990), and in batch reactors the ratio is about 3–6 (Ozturk & Palsson, 1991). Both glucose and glutamine function to provide energy and precursor metabolites for cell growth.

The goal of our next set of calculations is to determine how the differences in the catabolic pathway stoichiometries of glucose and glutamine can account for the observed consumption ratios. Also, the effects of flux capacity limitations on cell growth at different ratios of glucose to glutamine uptake rates are examined. Limitations on flux through the following reactions have been examined: MAL-ASP shuttle, pyruvate dehydrogenase (PDH), glutamate dehydrogenase (GLU-DH), αKG-DH, malic enzyme, and oxygen uptake rate. These reactions were selected because of the pivotal role that they are thought to perform in the catabolism of glutamine and glucose.

The network was constructed so that the cell could consume enough of the essential amino acids needed for biosynthesis, but the catabolic pathways were removed from the network. The uptake rates of non-essential amino acids were also removed from the network. The sum of the glucose and glutamine consumed was given the constant value of 150 nmol/10^6 cells hr^{-1}, and the maximal growth rate was calculated for q_{GLC}/q_{GLN} ratios between 0·1 and 10.

Figure 5(a) shows the maximum growth rates that were obtained as a function of q_{GLC}/q_{GLN} and oxygen uptake. At moderate oxygen uptake rates, the growth rate was maximum over the range of q_{GLC}/q_{GLN} equal to 2–7, which is similar to the experimentally observed values cited above. This result indicates that both glucose and glutamine are useful energy sources, although glucose has greater value than glutamine. The growth rate decreased at q_{GLC}/q_{GLN} greater than 7, due to nitrogen limitation. At lower q_{O_2}, the growth rate was slower, so that nitrogen limitation did not occur until q_{GLC}/q_{GLN} was greater than 10. When oxygen uptake was unlimited, the optimum q_{GLC}/q_{GLN} ratio was 1–2, indicating that under aerobic conditions, glutamine is nearly as valuable as glucose. The shadow prices for the calculations

FIG. 5. (a) Effect of q_{GLC}/q_{GLN} ratio on the maximum growth rate at different oxygen uptakes. q_{O_2} was set to (in nmol/10^6 cells hr^{-1}): (——), 140; (— —), 120; (- - -), 100; (— · —), unlimited oxygen uptake. The growth rate was normalized to 0·0275 hr^{-1}. No capacity restrictions were placed on any reactions. (b) The yield of ATP from glucose at $q_{O_2}=120$ (——), and 140 (— —), nmol/10^6 cells hr^{-1}. The yield of ATP from glutamine at $q_{O_2}=120$ (- - -), and 140, (— · —), nmol/10^6 cells hr^{-1}. (c) Effect on growth of capacity restrictions on: (——), control; (— —), glutamate dehydrogenase; (- - -), malate-aspartate shuttle; (— · —), pyruvate dehydrogenase; (· · · ·), and malic enzyme. The control has no capacity restrictions. The capacity of the individual reactions were limited to 50% of their calculated values in the control simulation. The glutamate dehydrogenase curve overlaps the control curve, and the malic enzyme curve overlaps the control curve for $q_{GLC}/q_{GLN}>2$. (d) Shadow prices for the calculations with unlimited oxygen uptake: (——), glutamine; (— —), G6P; (- - -), R5P.

with unlimited oxygen, shown in Fig. 5(d), demonstrate that the decreased growth rate at low q_{GLC}/q_{GLN} is due to limitation in pentose availability, while the limitation above q_{GLC}/q_{GLN} equal to two is due to limitation in amino group availability.

The yields of ATP per carbon atom for both glucose and glutamine at two oxygen uptake rates are shown in Fig. 5(b). At ratios of q_{GLC}/q_{GLN} less than 4, glutamine was a better energy source than glucose, since much of the glucose was metabolized anaerobically through the glycolytic pathway. At q_{GLC}/q_{GLN} above 6, the cell was limited for nitrogen, so that the energy yield from glutamine was slightly less than that from glucose. When q_{GLC}/q_{GLN} was less than 2, the ATP yield from glutamine dropped considerably because the cell growth was slow due to limitation by glucose, and thus the demand for ATP from glutamine was small. The ATP yield from glucose increased at the higher oxygen uptake rate, as expected, which allowed the cell to grow faster. However, the higher growth rate at the greater oxygen uptake caused more of the glutamine to be diverted for biosynthesis, so that the ATP yield from glutamine actually decreased as the oxygen uptake rate increased. The yield from glucose never approached the theoretical limit for aerobic conditions, because when glucose was no longer limiting for growth, the limitation for nitrogen caused cell growth to be slow and thus the demand for ATP to be low. At the physiological conditions of q_{GLC}/q_{GLN} equal to 6 and q_{O_2} equal to 120 nmol/10^6 cells hr^{-1} the ATP yields were similar for both glutamine and glucose.

Figure 5(c) illustrates the effects of constraints on the MAL-ASP shuttle, malic enzyme, GLU-DH, and pyruvate dehydrogenase at $q_{O_2} = 120$ mol/10^6 cells hr^{-1}. The simulation described as "control" was calculated with no capacity restrictions, and is the same as shown in Fig. 5(a). The capacity restrictions were set to 50% of the flux values calculated in the control simulation. We see from Fig. 5(c) that the MAL-ASP constraint caused the growth rate to have an optimum at $q_{GLC}/q_{GLN} = 4$. The constraint on the MAL-ASP shuttle limited the amount of glucose that could be oxidized; consequently, at q_{GLC}/q_{GLN} greater than 4, the extra glucose must be metabolized anaerobically, and the lack of oxidizable nutrients resulted in the reduction in growth rate. Restrictions on PYR-DH limited the growth rate at q_{GLC}/q_{GLN} greater than 2, since oxidation of glucose is prevented if pyruvate cannot be oxidized.

The growth rate was insensitive to restrictions on GLU-DH, suggesting that this enzyme does not need to be active in the cell in order for the cell to achieve its maximum growth rate. This result is consistent with the observations that activity of GLU-DH is much less than that of the GLU-transaminases extracted from lymphocytes (Ardawi & Newsholme, 1982) and tumor tissue (Glazer *et al.*, 1974), as well as from studies of glutamine metabolism in lymphocytes (Brand *et al.*, 1989) and tumor mitochondria (Moreadith & Lehninger, 1984). However, others have found GLU-DH to play an important role in glutamine catabolism in tumors (Kovacevic, 1971). The growth rate was slightly sensitive to the malic enzyme restriction only at high values of q_{GLN}. Sensitivity of growth rate to malic enzyme flux is expected since malic enzyme is found in most tumor tissues (McKeehan, 1986) where high rates of glutaminolysis occur.

In summary, we calculated a q_{GLC}/q_{GLN} ratio that was optimal for cell growth, and this ratio depended on the oxygen uptake rate as well as the MAL-ASP shuttle

capacity. At low q_{GLC}/q_{GLN}, growth is limited primarily by the availability of pentoses from glucose, and at high q_{GLC}/q_{GLN}, growth is limited by the availability of amino groups from glutamine. The GLU-DH reaction, whose role in glutamine metabolism is uncertain, was found to be unnecessary for efficient cell growth at all ratios of q_{GLC}/q_{GLN}.

Conclusions

The complexity of the metabolic network and the large number of kinetic parameters involved makes it difficult to mathematically model the cell's mass and energy metabolism with accuracy. The structure of the metabolic network is much better known than are the details of the kinetics of each enzyme participating in the network. By our analysis of the network stoichiometry, we do not introduce the error associated with kinetic models. On the other hand, we are unable to predict the behavior of the cell, in particular the distribution of fluxes within the metabolic network, with the same detail as one can with a kinetic model. In this paper, we presented the method of analysis of stoichiometry using linear optimization. We then demonstrated that linear optimization can yield useful information about the overall objective of cell metabolism, the interactions of nutrients with demands on the cell, the yields of energy and mass from nutrients, and the sensitivity of growth to limitations on various reactions.

The first section of this paper discussed the relevance of an objective function to cell metabolism. While no single objective can be said to govern cell behavior, the objective of minimizing redox production gave results most similar to actual hybridoma cell behavior.

The preference of the cell for glutamine as a nitrogen donor and as an energy supplier can be explained partly by the stoichiometric structure of the catabolic pathways. Glutamine, as well as the other amino acids that are catabolized directly to glutamate, gave the highest theoretical growth yields based on moles amino acid consumed, although proline and alanine yielded the most mass and energy on a per carbon basis. Glutamine was also calculated to be a preferred nutrient when NADH production was minimized and when glucose oxidation was limited by restrictions placed on the MAL/ASP shuttle. Additionally, the shadow prices have indicated that glutamine is a better nutrient than glutamate due to the difference in ATP value, rather than the difference in amino group content. Consequently, we concluded that at least part of the reason that glutamine is a preferred nutrient under *in vitro* conditions is due to the efficient structure of its catabolic pathway.

The relative values of glucose and glutamine as nutrients were compared by varying the ratio of q_{GLC}/q_{GLN} and calculating the maximum growth rate. The optimum value of the q_{GLC}/q_{GLN} ratio was between 2–7, similar to observed ratios. This result indicated that the observed q_{GLC}/q_{GLN} ratio may occur due to the structure of the catabolic pathways for glucose and glutamine. When oxygen uptake was unlimited, the optimum q_{GLC}/q_{GLN} ratio was 1–2, indicating that glutamine and glucose can have nearly equal value when oxygen is plentiful, although the calculated growth rate is much higher than what is practically achievable by the cell. We have found

that while certain reactions, such as malic enzyme and GLU-DH, are used for growth and metabolism, these reactions may be inhibited or deleted with little or no adverse effect on the calculated cell growth rate. To verify this result experimentally, one would have to delete the genes for these enzymes and then measure the resulting growth rate. Although we calculated that other reactions were able to replace these deleted reactions, the thermodynamics of the system may prevent this substitution from actually taking place.

The second part of this series will examine the stoichiometric structure of the hybridoma cell in more detail, using experimental measurements of metabolite fluxes into and out of the cell. Linear optimization will be used to interpret this data, and to elucidate the relationships between different nutrients and between energy and mass demands at physiological conditions.

The authors gratefully acknowledge support for this research from the National Science Foundation grant EET-8712756.

REFERENCES

ALBERTS, B., BRAY, D., LEWIS, J., RAFF, M., ROBERTS, K. & WATSON, J. D. (1983). *Molecular Biology of the Cell.* Garland Publishing.

ARDAWI, M. & NEWSHOLME, E. A. (1982). Maximum activities of some enzymes of glycolysis, the tricarboxylic acid cycle and ketone-body and glutamine utilization pathways in lymphocytes of the rat. *Biochem. J.* **208,** 743–748.

BAILEY, J., HOWARD, B., DUNBAR, L. & TILLMAN, S. (1972). Control of lipid metabolism in cultured cells. *Lipids* **7,** 125–134.

BEAVIS, A. D. & LEHNINGER, A. L. (1986). The upper and lower limits of the mechanistic stoichiometry of mitochondrial oxidative phosphorylation. *Eur. J. Biochem.* **158,** 315–322.

BLUM, J. J. & STEIN, R. B. (1982). On the analysis of metabolic networks. In: *Biological Regulation and Development* Vol. 3A (Goldberger, R. & Yamamoto, K., eds) pp. 99–125. New York: Plenum Press.

BRAND, K., FEKL, W., VON HINTZENSTERN, J., LANGER, K., LUPPA, P. & SCHOERNER, C. (1989). Metabolism of glutamine in lymphocytes. *Metabolism* **38**(8, Suppl. 1), 29–33.

CRAWFORD, J. M. & BLUM, J. J. (1983). Quantitative analysis of flux along the gluconeogenic, glycolytic and pentose phosphate pathways under reducing conditions in hepatocytes isolated from fed rats. *Biochem. J.* **212,** 595–598.

CREIGHTON, T. E. (1984). *Proteins: Structures and Molecular Principles.* San Francisco: W.H. Freeman.

DARNELL, J. E. (1976). mRNA structure and function. *Prog. Nucl. Acid Res. Molec. Biol.* **19,** 493–511.

EAGLE, H. & LEVINTOW, L. (1965). Amino acid and protein metabolism. I. The metabolic characteristics of serially propagated cells. In: *Cells and Tissues in Culture* Vol. I (Willmer, E., ed.) pp. 277–296. New York: Academic Press.

EIGENBRODT, E., FISTER, P. & REINACHER, M. (1985). New perspectives on carbohydrate metabolism in tumor cells. In: *Regulation of Carbohydrate Metabolism* Vol. II (Baitner, R., ed.) pp. 141–179. Boca Raton, FL: CRC Press.

FELL, D. A. & SMALL, J. R. (1986). Fat synthesis in adipose tissue: an examination of stoichiometric constraints. *Biochem. J.* **238,** 781–786.

FLEISCHAKER, R. J. (1986). Practical matters in instrumentation for mammalian cell cultures. In: *Mammalian Cell Technology* (Thilly, W. G., ed.) pp. 199–211. Oxford, U.K.: Butterworths.

GLAZER, R., VOGEL, C., POTEL, I. & ANTHONY, P. (1974). Glutamate dehydrogenase activity related to histopathological grade of hepatocellular carcinoma in man. *Cancer Res.* **34,** 2975.

GREENHOUSE, W. V. & LEHNINGER, A. L. (1976). Occurrence of the malate-aspartate shuttle in various tumor types. *Cancer Res.* **36,** 1392–1396.

HOLMS, W. (1986). The central metabolic pathways of *Escherichia coli*: relationship between flux and control at a branch point, efficiency of conversion to biomass, and excretion of acetate. *Curr. Top. Cell. Regul.* **28,** 69–105.

INGRAHAM, J. L., MAALOE, O. & NEIDHARDT, F. C. (1983). *Growth of the Bacterial Cell.* Sunderland, MA: Sinauer Associates.

KILBURN, D., LILLY, M. & WEBB, F. (1969). The energetics of mammalian cell growth. *J. Cell Sci.* **4,** 645–654.

KOVACEVIC, Z. (1971). The pathways of glutamine and glutamate oxidation in isolated mitochondria from mammalian cells. *Biochem. J.* **125,** 757.

LEMASTERS, J. (1984). The ATP-to-oxygen stoichiometries of oxidative phosphorylation by rat liver mitochondria. An analysis of ADP-induced oxygen jumps by linear nonequilibrium thermodynamics. *J. biol. Chem.* **259,** 13123–13130.

LOPEZ-ALARCON, L., EBOLI, M., DE LIBERALI, E., PALOMBINI, G. & GALEOTTI, T. (1979). Evidence for the oxidation of glycolytic NADH by the malate-aspartate shuttle in Ehrlich ascites tumor cells. *Arch. Biochem. Biophys.* **192**(2), 391–395.

LUENBERGER, D. G. (1984). *Linear and Nonlinear Programming*. NJ: Addison-Wesley.

MAJEWSKI, R. & DOMACH, M. (1990). Simple constrained-optimization view of acetate overflow in *E. coli*. *Biotechnol. Bioengng.* **35,** 732–738.

MCKEEHAN, W. L. (1986). Glutaminolysis in animal cells. In: *Carbohydrate Metabolism in Cultured Cells* (Morgan, M. J., ed.) pp. 111–150. New York: Plenum.

MILLER, W., WILKE, C. & BLANCH, H. (1988*a*). *Transient and steady-state responses in continuous hybridoma culture*. Presentation at the American Chemical Society National Meeting, Los Angeles, CA.

MILLER, W., WILKE, C. & BLANCH, H. (1988*b*). Transient responses of hybridoma metabolism to changes in the oxygen supply rate in continuous culture. *Bioprocess Engng.* **3,** 1–9.

MILLER, W. M., WILKE, C. & BLANCH, H. (1986). *Hybridoma responses to nutrient pulse and step changes in continuous culture. Implications for metabolic regulation*. Presentation at the American Institute of Chemical Engineers National Meeting.

MOREADITH, R. W. & LEHNINGER, A. L. (1984). The pathways of glutamate and glutamine oxidation by tumor cell mitochondria. Role of mitochondrial $NAD(P)^+$-dependent malic enzyme. *J. biol. Chem.* **259**(10), 6215–6221.

NIRANJAN, S. & SAN, K. -Y. (1989). Analysis of a framework using material balances in metabolic pathways to elucidate cellular metabolism. *Biotechnol. Bioengng.* **34,** 496–501.

OZTURK, S. S. & PALSSON, B. O. (1990). Effects of dissolved oxygen on hybridoma cell growth, metabolism, and antibody production kinetics in continuous culture. *Biotech. Prog.* **6,** 437–446.

OZTURK, S. S. & PALSSON, B. O. (1991). Growth metabolic, and antibody production kinetics of hybridoma cell culture: II effects of serum concentration, dissolved oxygen concentration, and medium pH in a batch reactor. *Biotech. Prog.* **7,** 481–494.

PAPOUTSAKIS, E. T. & MEYER, C. L. (1985). Equations and calculations of product yields and preferred pathways for butanediol and mixed-acid fermentations. *Biotechnol. Bioengng.* **27,** 50–66.

PEREZ-RODRIGUEZ, J., SANCHEZ-JIMINEZ, F., MARQUEZ, F. J., MEDINA, M. A., QUESADA, A. R. & DE CASTRO, I. N. (1987). Malate-citrate cycle during glycolysis and glutaminolysis in Ehrlich ascites tumor cells. *Biochimie* **69,** 469–474.

PIRT, S. (1982). Maintenance energy: a general model for energy-limited and energy-sufficient growth. *Arch. Microbiol.* **133,** 300–302.

RABKIN, M. & BLUM, J. (1985). Quantitative analysis of intermediary metabolism in hepatocytes incubated in the presence and absence of glucagon with a substrate mixture containing glucose, ribose, fructose, alanine and acetate. *Biochem. J.* **225,** 761–786.

RUDLAND, P., WEIL, S. & HUNTER, A. (1975). Changes in RNA metabolism and accumulation of presumptive messenger RNA during transition from the growing to the quiescent state of cultured mouse fibroblasts. *J. molec. Biol.* **96,** 745–766.

SAFER, B. & WILLIAMSON, J. (1973). Mitochondrial and cytosolic interactions in perfused rat heart. Role of coupled transamination in repletion of citric acid cycle intermediates. *J. biol. Chem.* **248**(7), 2570–2579.

SAUER, F., ERFLE, J. & BINNS, M. (1970). Turnover rates and intracellular pool size distribution of citrate cycle intermediates in normal, diabetic and fat-fed rats estimated by computer analysis from specific activity decay data of ^{14}C-labeled citrate cycle acids. *Eur. J. Biochem.* **17,** 350–363.

SAVINELL, J. M. & PALSSON, B. O. (1991). Network analysis of intermediary metabolism using linear optimization. II. Interpretation of hybridoma cell metabolism. *J. theor. Biol.* **154,** 455–473.

STUCKI, J. W. & WALTER, P. (1972). Pyruvate metabolism in mitochondria from rat liver: measured and computer-simulated fluxes. *Eur. J. Biochem.* **30,** 60–72.

THOMAS, J. N. (1986). Nutrients, oxygen, and pH. In: *Mammalian Cell Technology* (Thilly, W., ed.) pp. 109–130. Oxford, U.K.: Butterworths.

TSAI, S. & LEE, Y. (1988). Application of Gibbs' rule and a simple pathway method to microbial stoichiometry. *Biotechnol. Prog.* **4**(2), 82–88.

WALSH, K. & KOSHLAND, D. E. (1985). Branch point control by the phosphorylation state of isocitrate dehydrogenase. *J. biol. Chem.* **260**(14), 8430–8437.

APPENDIX

Antibody Glycosylation

Using an average structure for the carbohydrate (CHO) chain of the antibody molecule, the dolichol cycle for the synthesis of the initial carbohydrate chain is shown in Fig. A1(a). The addition of the carbohydrate group to the antibody, the trimming of the carbohydrate group, and the addition of sugar groups are shown in Fig. A1(b).

The general equation for charging the sugar molecule with uridine triphosphate (UTP) is given by:

$$\text{sugar} + \text{UTP} + \text{ATP} \rightarrow \text{sugar-UDP} + \text{ADP} + \text{PP}_i \qquad \text{(A.1)}$$

Similarly, the equation to charge the sugar with guanosine triphosphate (GTP) is:

$$\text{sugar} + \text{GTP} + \text{ATP} \rightarrow \text{sugar-GDP} + \text{ADP} + \text{PP}_i \qquad \text{(A.2)}$$

The formation of the sugar bound to P-DOL is given by:

$$\text{sugar-UDP} + \text{P-DOL} \rightarrow \text{sugar-P-DOL} + \text{UDP} \qquad \text{(A.3)}$$

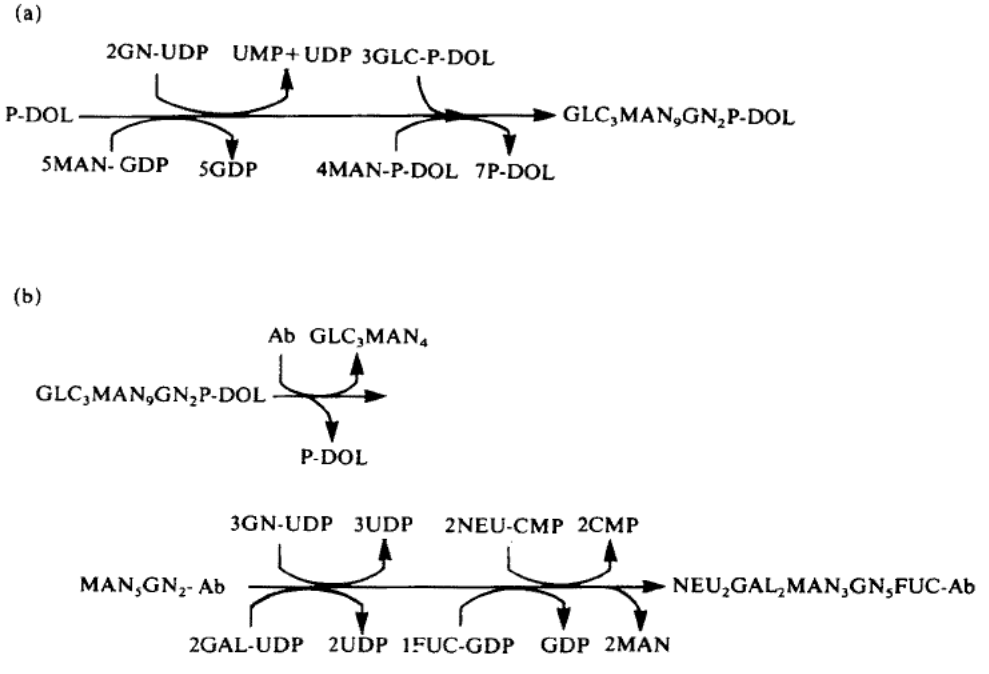

FIG. A1. Glycosylation of the antibody heavy chain. (a) The addition of the sugar groups to the lipid carrier, P-DOL. (b) Transfer of the carbohydrate chain from the P-DOL to the antibody, and subsequent additions and removal of sugar groups. Abbreviations are: Ab: antibody; CMP: cytidine monophosphate; FUC: fucose; GAL: galactose; GDP: guanosine diphosphate; GLC: glucose; GN: glucosamine; MAN: mannose; NEU: neuraminic acid; P-DOL: dolichyl monophosphate; UDP: uridine diphosphate; UMP: uridine monophosphate; UTP: uridine triphosphate.

By combining eqns (A.1–A.3), and the stoichiometry of the reactions shown in Fig. A1, the overall stoichiometry of the Ab glycosylation (for one heavy chain of the antibody) is given by:

$$\mathrm{Ab} + 3\mathrm{MAN} + 2\mathrm{GN} + 2\mathrm{GAL} + 1\mathrm{FUC} + 2\mathrm{NEU} + 45\mathrm{ATP} \rightarrow \mathrm{Ab_{CHO}} + 45\mathrm{ADP} + 22\mathrm{PP_i} \tag{A.4}$$

If we assume that each of these sugars is stoichiometrically equivalent to one glucose molecule, then one carbohydrate chain requires 13 GLC and 45 ATP. If the starting point from the network is G6P rather than GLC, then the requirement becomes 13 G6P and 32 ATP per carbohydrate chain. In general, only the heavy chains of the Ab molecule is glycosylated, so that there are two carbohydrate chains per complete Ab molecule. The G6P and ATP coefficients are then 26 G6P and 64 ATP per complete Ab molecule. To be consistent with the units of amino acids used for protein synthesis, the average stoichiometric coefficients for G6P and ATP are found from:

$$\frac{26\ \text{nmol G6P}}{\text{nmol Ab}} \cdot \frac{\text{nmol Ab}}{1300\ \text{nmol AA}} = 0{\cdot}020\ \frac{\text{G6P}}{\text{nmol AA}} \tag{A.5}$$

$$\frac{64\ \text{nmol ATP}}{\text{nmol Ab}} \cdot \frac{\text{nmol Ab}}{1300\ \text{nmol AA}} = 0{\cdot}049\ \frac{\text{ATP}}{\text{nmol AA}} \tag{A.6}$$

Nucleotide Synthesis

The flux through the nucleotide synthesis pathway needed for cell growth is shown in Table 2. However, the actual flux through the reaction that polymerizes the nucleotides into RNA is much higher due to the turnover of RNA, and the large amount of processing that is done to RNA before it leaves the nucleus. The calculation of the nucleotide polymerization and degradation rates are shown here.

The mass balances on mRNA, rRNA, NMP, and total RNA are:

$$\frac{\mathrm{d[mRNA]}}{\mathrm{d}t} = v_m - f_m \cdot v_m - (k_m + \mu) \cdot [\mathrm{mRNA}] \tag{A.7}$$

$$\frac{\mathrm{d[rRNA]}}{\mathrm{d}t} = v_r - f_r \cdot v_r - (k_r + \mu) \cdot [\mathrm{rRNA}] \tag{A.8}$$

$$\frac{\mathrm{d[NMP]}}{\mathrm{d}t} = v_{\mathrm{NMP}} - v_r - v_m + 0{\cdot}95 \cdot v_m + k_m \cdot [mRNA] + k_r \cdot [\mathrm{rRNA}] \tag{A.9}$$

$$\frac{\mathrm{d[RNA]}}{\mathrm{d}t} = v_m + v_r - \mu \cdot [\mathrm{RNA}] - v_{\mathrm{degr}} \tag{A.10}$$

where v_m is the synthesis rate of mRNA, v_r is the synthesis rate of rRNA, k_m is the degradation rate constant of mRNA, k_r is the degradation rate constant of rRNA, f_m and f_r are the fractions of mRNA and rRNA, respectively, that are degraded before the RNA leaves the nucleus, v_{degr} is the rate of total RNA degradation, due

to both nuclear processing and turnover. Approximately 95% of mRNA and 50% of rRNA are degraded in the nucleus ($f_m = 0{\cdot}95$, $f_r = 0{\cdot}50$) (Alberts *et al.*, 1983). The average half-life of mRNA is 16 hr (Darnell, 1976), and 60 hr for rRNA (Rudland *et al.*, 1975), yielding $k_m = 0{\cdot}043\ \mathrm{hr}^{-1}$ and $k_r = 0{\cdot}012\ \mathrm{hr}^{-1}$. The amount of rRNA is about 75%, tRNA is 15%, and mRNA is 10% of total RNA (Alberts *et al.*, 1983).

At steady state, the above derivatives are set equal to zero in order to calculate the flux v_{degr} for use in the network calculations. Using the amount of RNA in a cell with a 12 μm diameter cell shown in Table 2, and assuming a doubling time of 25 hr, the flux through v_{degr} is $5{\cdot}0\ \mathrm{nmol}/10^6\ \mathrm{cells\ hr}^{-1}$.